

3D geological reconstruction of the M. Vettore seismogenic fault system (Central Apennines, Italy): Cross-cutting relationship with the M. Sibillini thrust

Massimiliano Porreca^{a,*}, Andrea Fabbrizzi^{b,c}, Salvatore Azzaro^a, Stefano Pucci^d, Luca Del Rio^e, Pietro Paolo Pierantoni^f, Claudia Giorgetti^a, Gerald Roberts^g, Massimiliano Rinaldo Barchi^a

^a Dipartimento di Fisica e Geologia, Università di Perugia (CRUST Member, Centro interUniversitario per l'analisi SismoTettonica tridimensionale con applicazioni territoriali), Via Pascoli, 06123, Perugia, Italy

^b Department of Geological Sciences, San Diego State University, San Diego, CA, USA

^c Scripps Institution of Oceanography, University of California, San Diego, La Jolla, CA, USA

^d Istituto Nazionale di Geofisica e Vulcanologia, Via di Vigna Murata 605, 00143, Rome, Italy

^e Dipartimento di Geoscienze, Università di Padova, Via G. Gradenigo 6, 35131, Padova, Italy

^f Scuola di Scienze e Tecnologie, Università di Camerino, Via Gentile III da Varano, 62032, Camerino, MC, Italy

^g Department of Earth and Planetary Sciences, Birkbeck University of London, Malet St., WC1E 7HX, London, UK

ARTICLE INFO

Keywords:

2016-2017 Central Italy earthquake
Apennines
Cross-cutting relationships
Inherited structures
3D structural model

ABSTRACT

The 2016–2017 Amatrice-Norcia seismic sequence was triggered by the reactivation of a complex NNW-SSE trending, WSW-dipping normal fault system cross-cutting the Umbria-Marche fold and thrust belt near M. Vettore. This fault system produced clear and impressive co-seismic ruptures on normal faults in the hangingwall of the M. Sibillini thrust, whereas ruptures in the footwall were observed, but less clear. As a result, a strong controversy exists in the literature about the geometry of the seismogenic faults, their relationships with pre-existing thrusts, and the location of normal-faulting rupture tips. In this work, we present a 3D geological model of the M. Vettore area located between the Castelluccio basin and the outcrop of the M. Sibillini thrust, where the most evident co-seismic ruptures have been observed. The model shows the relationship between the ruptured normal faults and the M. Sibillini thrust, and was constructed using a grid of 14 geological cross-sections parallel and orthogonal to the main structural elements (i.e. normal faults and thrusts) down to a depth of 3 km. The model was built using reference structural surfaces, such as the top of the Early Cretaceous Maiolica Fm., the M. Sibillini thrust and the main seismogenic normal faults belonging to the M. Vettore fault system. The 3D model has allowed us to calculate the vertical cumulative throw distribution for the M. Vettore normal faults. The cumulative geological throw of ca. 1300 m across the normal faults in the proximity of the M. Sibillini thrust indicates that the seismogenic fault system continues into the footwall of the thrust, displacing it in the sub-surface. The results of this study provide important constraints on the cross-cutting relationships between active normal and pre-existing compressional structures in seismically active areas, contributing to a better definition of the faults segmentation, and the related seismic hazard.

1. Introduction

In geologically complex areas, the geometry and segmentation of seismogenic faults may be affected by pre-existing structures. Inherited and favorably oriented structures may be either reactivated in the new tectonic regime, or may act as barriers to rupture propagation, controlling the segmentation of the active fault system (e.g. Schwartz and

Sibson, 1989; Crone and Haller, 1991; Collettini et al., 2005). Possible control on active normal faults posed by pre-existing thrusts is relevant for the active extensional belt of the Central Apennines, where a set of NNW-SSE trending normal faults, active since the Early Quaternary and responsible of the seismicity of the region (e.g. Lavecchia et al., 1994; Calamita et al., 1994a; Ferrarini et al., 2015), affects the arc-shaped, Late Miocene-Early Pliocene structures of a pre-existing fold and

* Corresponding author.

E-mail address: massimiliano.porreca@unipg.it (M. Porreca).

thrust belt (e.g. Lavecchia et al., 1994; Calamita et al., 1994a).

In 2016 and 2017 the Central Apennines were affected by a seismic sequence, triggered by activation of a NNW-SSE trending normal fault system. The epicentral area, as depicted by the recorded seismicity, extends about 70 km in NNW-SSE direction (e.g. Chiaraluce et al., 2017, Fig. 1) crossing a complex region consisting of two different

structural/geological domains affected by thrusts (Fig. 1): the Umbria-Marche domain, where Mesozoic-Neogene carbonates crop-out; and the Laga domain, where the same succession is covered by a thick siliciclastic foredeep succession (e.g. Koopman et al., 1983; Lavecchia, 1985; Centamore et al., 1992). The two domains are tectonically separated by the M. Sibillini thrust (MSt) (Fig. 1).

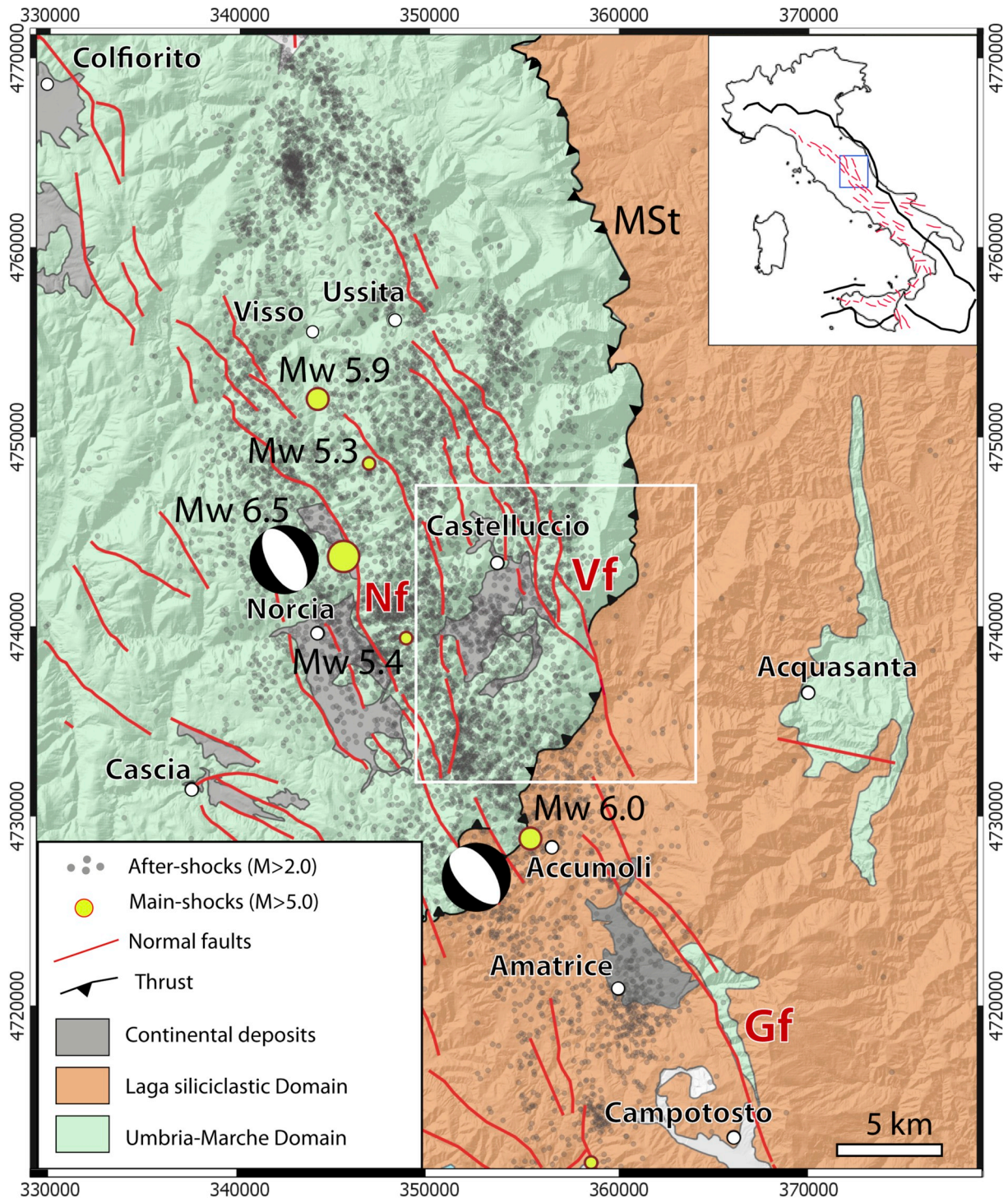


Fig. 1. Structural map of the Umbria-Marche Apennines affected by the 2016–2017 seismic sequence. The map highlights the main geological domains and the structural relationship between NNW-SSE-striking normal faults and the arcuate M. Sibillini thrust (MSt). The four main-shocks (Mw 6.0 August 24th, 2016; Mw 5.4 August 24th, 2016; Mw 5.4 October 26th, 2016; Mw 5.9 October 26th, 2016; Mw 6.5 October 30th, 2016) and after-shock distribution (Mw > 2.0) are reported in the map, together with the two focal mechanisms of the M ≥ 6.0 events. The seismic data are from Chiaraluce et al. (2017). In the inset, a schematic tectonic map of Italy with the main thrust (thick black lines) and normal faults (red lines). MSt: M. Sibillini thrust; Vf: M. Vetture fault system; Gf: Gorzano fault system; Nf: Norcia fault system. (For interpretation of the references to colour in this figure legend, the reader is referred to the Web version of this article.)

The seismic sequence started on August 24th 2016 with the Mw 6.0 mainshock located north of the town of Amatrice (Amatrice earthquake). The mainshock nucleated along a SW-dipping normal fault belonging to the northern segment of the M. Gorzano fault (Gf) with an epicenter located within the siliciclastic Laga domain (Tinti et al., 2016; Lavecchia et al., 2016). During this event, primary co-seismic ruptures were observed along the M. Vettore fault system (Vf) in the carbonate Umbria-Marche domain above the MSt (Livio et al., 2016; Pucci et al., 2017; Brozzetti et al., 2019). In contrast, along the well-known active Gf, coseismic ruptures were discontinuous or absent, and hence of equivocal origin (Livio et al., 2016; Emergeo Working Group, 2017). On October 26th a Mw 5.9 earthquake nucleated to the north of the Vf, close to the town of Visso (Visso earthquake). The seismic sequence continued on October 30th with a Mw 6.5 earthquake, north to the Norcia town (Norcia earthquake), due to the reactivation of the Vf (Chiaraluca et al., 2017). Along this fault system, located in the hangingwall of the MSt, impressive primary coseismic ruptures formed due to surface faulting (Ferrario and Livio, 2018; Iezzi et al., 2018; Villani et al., 2018a; Perouse et al., 2018; Brozzetti et al., 2019). Coseismic displacements (an average of ca. 0.44 m and peak of ca. 2.1 m) were observed for a total length of ca. 27 km with N135°-160° striking surface ruptures. These ruptures show prevalent dip slip kinematics denoting an extension axis trending SW-NE (N233°, Villani et al., 2018a; Brozzetti et al., 2019), which is consistent with both structural (Brozzetti and Lavecchia, 1994; Calamita et al., 1994a, 2000; Civico et al., 2018) and seismological data (Albano et al., 2016; Tinti et al., 2016; Chiaraluca et al., 2017; Scognamiglio et al., 2018). The southern tip of the coseismic surface ruptures, although less continuous along strike within colluvial deposits than further to the NW, appear to cross the pre-existing MSt and extends 2–3 km in its footwall block (Pucci et al., 2017; Civico et al., 2018; Villani et al., 2018a; Brozzetti et al., 2019).

The role of major inherited structures, such as the MSt, in controlling the mainshocks nucleation and/or segmentation of the seismogenic normal faults of the region is widely debated in the literature, based on the controversial cross-cutting relationships between the active normal faults and the MSt (Bally et al., 1986; Calamita et al., 1994a; Lavecchia et al., 1994, 2016; Coltorti and Farabollini, 1995; Mazzoli et al., 2005; Pierantoni et al., 2005; Pizzi and Galadini, 2009; Pizzi et al., 2017; Brozzetti et al., 2019). The main point of the discussion is represented by the fault segmentation in the area of the MSt, that is, if the thrust acted as a barrier or not to the co-seismic slip propagation during the 2016–2017 seismic sequence.

Before this last seismic sequence, different authors suggested that Quaternary normal faults do not displace the MSt, but detached at depth on the low-angle thrust surface (Bally et al., 1986; Calamita et al., 1994a) with a displacement that abruptly decreases near the intersection with the MSt (Pizzi and Galadini, 2009).

After the 2016–2017 seismic sequence and the first results on the seismicity distribution, other interpretations were proposed to support the hypothesis on the role of the inherited structures in controlling the activation of seismogenic faults. In particular, Bonini et al. (2016) suggest that a 30°-40°-dipping ramp of the MSt, in the uppermost 6 km of the crust, was reactivated with extensional kinematics acting as a west-dipping detachment fault. A similar interpretation was given by Pizzi et al. (2017) who suggest a segmentation of seismogenic sources controlled by inherited discontinuities, such as the MSt.

In contrast, other studies suggested that the normal fault systems of Central Italy crosscut the pre-existing late Miocene fold and thrust belt, including the main inherited structures such as the MSt (Brozzetti and Lavecchia, 1994; Lavecchia et al., 1994, 2016; Coltorti and Farabollini, 1995; Roberts and Michetti, 2004; Mazzoli et al., 2005; Pierantoni et al., 2005; Porreca et al., 2018; Iezzi et al., 2018). Also, Calamita et al. (1994b) suggest that some normal faults may cross-cut the thrusts, whereas other faults are detached at shallower levels promoting tectonic inversion of pre-existing thrusts. Recently, Brozzetti et al. (2019) performed detailed field work focused on the surface ruptures of the M.

Vettore area. They propose that the Vf displaces westward the MSt with a throw of ca. 300 m, and that the Vf continues southward in the footwall of the MSt, affecting the siliciclastic Laga Fm.

This debate is long-lived, for example in geological maps, starting from the Geological Map of Italy by Scarsella et al. (1941), where the trace of the MSt is not affected by normal faults, which are rarely represented by the authors. More recent maps, such as those of Centamore et al. (1992) and Pierantoni et al. (2013), also show that the MSt is continuous in proximity to the southern termination of the Vf. In contrast, Boccaletti and Coli (1982) and Lavecchia et al. (1985) produced structural geological maps of the Northern Apennines and the MSt respectively, where the MSt is shown to be displaced by the Vf. Thus, there is an ongoing debate about the role of the MSt, because the area where Vf intersects the MSt is partly covered by thick detrital deposits, hampering the direct observation of the cross-cutting relationships (Pierantoni et al., 2013). A clarification about the geometrical and kinematic relationships between Vf and MSt is therefore necessary to gain insights into the segmentation and lengths of seismogenic faults with obvious implications on the maximum expected magnitude according to the scaling relationships (e.g. Wells and Coppersmith, 1994; Leonard, 2010; Stirling et al., 2013). This study focuses on the controversial geometrical relationship between the seismogenic faults and older inherited structures. We define: (1) the 3D reconstruction of the MSt and of the seismogenic Vf, as well as their cross-cutting relationships; (2) the throw distribution along the Vf strike and its implications on the southern termination of Vf, within the siliciclastic Laga domain; (3) the comparison between long-term (geological) and short-term (coseismic) offset of the Vf.

2. Geological setting

The Neogene-Quaternary evolution of the central Apennines is the result of the contemporaneous opening of the Tyrrhenian sea, the eastward migration of a compressive front and the flexural retreat of the Adriatic lithospheric plate (Boccaletti et al., 1982; Malinverno and Ryan, 1986; Royden et al., 1987; Patacca et al., 1990; Doglioni et al., 1994; Di Bucci and Mazzoli, 2002; Molli, 2008; Carminati and Doglioni, 2012). Most of the mountain ridge of the study area corresponds to the Umbria-Marche fold and thrust belt. The structural evolution of this region is characterized by a Late Miocene-Early Pliocene compressional phase, followed by Late Pliocene-Quaternary extension (e.g., Pauselli et al., 2006; Barchi, 2010; Cosentino et al., 2010, 2017).

2.1. Stratigraphic setting

The geological formations exposed in the study area belong to the well-known Mesozoic-Paleogene Umbria-Marche succession (e.g. Centamore et al., 1986; Cresta et al., 1989) and to the overlying turbidites of the Laga Fm. (e.g. Centamore et al., 1992), extensively cropping out in the footwall of the MSt (i.e. Laga Domain in Fig. 1). For the purposes of this study, this geologically complex succession has been schematically divided into 6 main Units, as shown in Fig. 2.

The lower part of the succession (Late Triassic-Paleogene) reflects the tectono-sedimentary evolution of a continental passive margin, where shallow-water marine sediments (Evaporites Unit and shallow-water Carbonates Unit) are followed by a deeper, pelagic, largely carbonate multilayer (Basinal Unit and Scaglia Unit). The deposition of the hemipelagic, pre-turbiditic successions of the Marly Unit (Miocene) marks the end of the divergent environment and the transition towards the onset of a proper syn-convergent foreland basin, where the thick siliciclastic Laga Unit was deposited in the Messinian (Milli et al., 2007).

As also illustrated in Fig. 2, the Basinal Unit is characterized by remarkable lateral variability, reflecting the effects of extensional, syn-sedimentary tectonics (e.g. Colacicchi et al., 1970; Alvarez, 1989; Santantonio, 1994; De Paola et al., 2007). During this phase, structural highs, capped by reduced thickness of sediments (condensed succession,

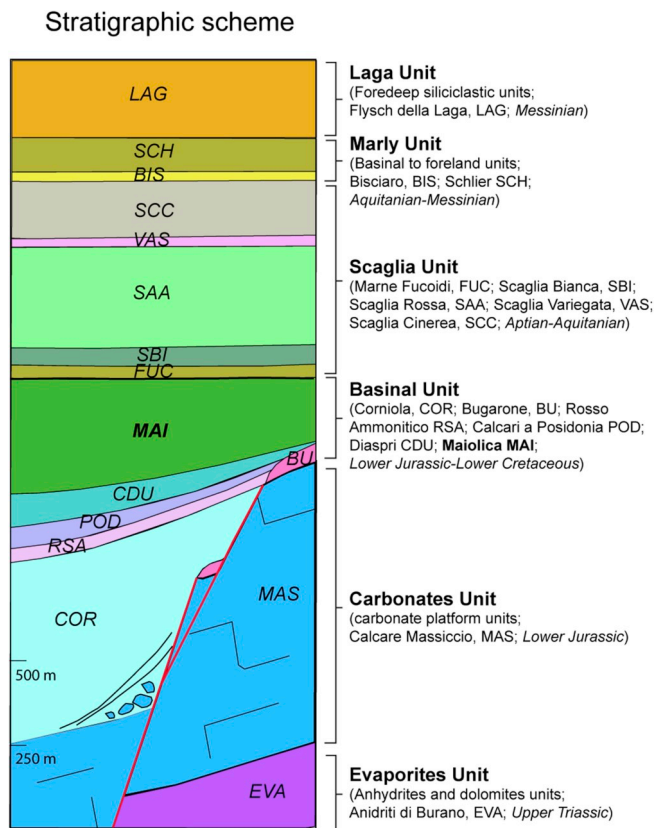


Fig. 2. Stratigraphic scheme of the M. Vettore area. The thickness variations are inferred by published data of Pierantoni et al. (2013). The formations are grouped to six main Units in order to simplify the construction of the 3D geological model. The top of Maiolica Fm. (MAI) was used as reference surface for constructing the 3D geological model of this study.

i.e. Bugarone Fm.), were separated by deep troughs where Jurassic sediments show their maximum thickness (complete succession, i.e. Corniola, Marne del Serrone, Rosso Ammonitico, Calcarei a Posidonia, Calcarei Diaspri Formations). This configuration is clearly documented in the studied area, as mapped by Pierantoni et al. (2013). At the Jurassic/Cretaceous boundary, the paleotopography, related to the syn-sedimentary extensional phase, was buried and eroded during the deposition of the Maiolica Fm. For this reason, we use the top of the Maiolica Fm. as structural surface in our 3D reconstruction to avoid any complication related to the Jurassic extensional tectonic phase.

2.2. Structural setting

The stratigraphic multilayer described above was deformed during the Miocene compressional phase, giving rise to the Umbria-Marche fold and thrust belt. The compressional structures show typical thrust belt morphologies whose geometries are well documented in the literature (Koopman, 1983; Lavecchia, 1985; Centamore et al., 1992; Calamita et al., 1994a; Mazzoli et al., 2005; Pierantoni et al., 2005, 2013; Tavani et al., 2008). These well-known geometries facilitate calculation of the fault-related offsets. In the study area, the Umbria-Marche sequence overthrusts the Laga Fm., through the arc-shaped MSt (Koopman, 1983; Lavecchia, 1985), with eastward convexity. The tectonic style is characterized by significant displacements across the main thrusts of several kilometres, with a progressive sequence in age of compressional structures toward the foreland (i.e., toward the ENE). The main detachment is localized at the base of the Triassic evaporites sequence and involves the whole sedimentary sequence deformed in NE verging thrust anticlines. These anticlines are characterized by overturned forelimbs and

gently west dipping backlimbs, associated with outcropping or blind thrusts. The siliciclastic foredeep sequence outcrops only to east of the MSt and is strongly deformed with frequent low-amplitude folds (Koopman, 1983; Porreca et al., 2018 and references therein).

Since the Late Pliocene, extensional tectonics has cross-cut the compressional structures. NW-SE trending normal faults have been responsible for the formation of large intermontane basins in which Late Pliocene-Quaternary continental sediments were deposited. Evidence of activity in the last 2 Ma (Calamita et al., 1994b; Cavinato and De Celles, 1999; Roberts and Michetti, 2004) is given by the strong link between the topography and displacements along the main normal faults.

2.3. The M. Vettore area and active faults

M. Vettore represents the highest elevation of the whole Umbria-Marche Apennines. The geology is characterised by the Castelluccio basin to the west and MSt to the east (Fig. 3). The MSt shows an arcuate shape, changing its strike from NNW-SSE in the northern sector to NNE-SSW in the southern sector with respect to the M. Vettore (Calamita et al., 2003; Di Domenica et al., 2012; Boccaletti et al., 2005; Finetti et al., 2005). In proximity of the M. Vettore, the MSt has prevalent N-S strike, with a low angle westward dip (Lavecchia, 1985).

M. Vettore provides extensive exposures of Jurassic successions (particularly on its eastern slope), revealing a clear unconformity separating the Corniola Fm. from the Calcare Massiccio Fm. The MSt juxtaposes the Meso-Cenozoic carbonate succession, deformed by an east-verging asymmetric anticline, onto the Messinian siliciclastic foredeep deposits (Laga Fm.) (Pierantoni et al., 2013; Di Domenica et al., 2012). To the east of the MSt, the structural setting of the footwall consists of a set of small-wavelength folds (ca. 0.5–2 km), involving different members of the Laga Fm. These folds show different sizes and lengths (3–10 km along-axis elongation) and are characterized by a shallow detachment (ca. 1–2 km of depth) probably located within the hemipelagic pre-turbiditic Marly Unit (“Laga Detachment Zone”, Koopman, 1983).

The Quaternary extensional phase produced high-angle normal faults, with prevalent dip-slip and, subordinately, oblique kinematics (Brozzetti and Lavecchia, 1994; Pizzi and Scisciani, 2000; Pizzi et al., 2002). The average strike of the normal faults is N150°, that is oblique to the N-S to NE-SW-trending Neogene compressional structures (i.e. fold axes and thrust faults) (Fig. 3). In particular, the NNW-SSE-trending M. Vettore normal fault system extends for about 30 km in length, from the Tronto river valley to the SE, to Ussita village to the NW (Pizzi et al., 2002; Iezzi et al., 2018) (Fig. 1). It comprises synthetic WSW-dipping fault splays, with an en-échelon geometry, locally connected to each other by transfer faults and minor antithetic splays (Pizzi et al., 2002; Galadini and Galli, 2003; Pizzi and Galadini, 2009; Ercoli et al., 2014; Villani et al., 2018b). The seismicity that affected this area since the August 24th 2016 was attributed to the activation of the entire fault system (Civico et al., 2018). Considering the evidence of paleo-earthquakes and the lack of historical earthquakes associated, the Vf system was considered “silent” before the last seismic crisis (Galadini and Galli, 2000), with palaeoseismology suggesting that the previous earthquakes on this system occurred with a long elapsed time (a return time to 1800 ± 300 years for events with $M_w > 6.6$ was recently estimated by Galli et al., 2019).

The normal Vf system is also responsible of the formation and evolution of the Quaternary Castelluccio basin, located on the hangingwall of the MSt (Fig. 3). This intramontane basin is one of the easternmost tectonic depressions of the Umbria-Marche Apennines. The basin is characterized by a NNE-SSW elongated, rectangular-shaped geometry (Coltorti and Farabollini, 1995; Villani et al., 2018b), and filled by coarse-grained alluvial and lacustrine deposits with a maximum estimated thickness of ca. 250 m (Villani et al., 2018b).

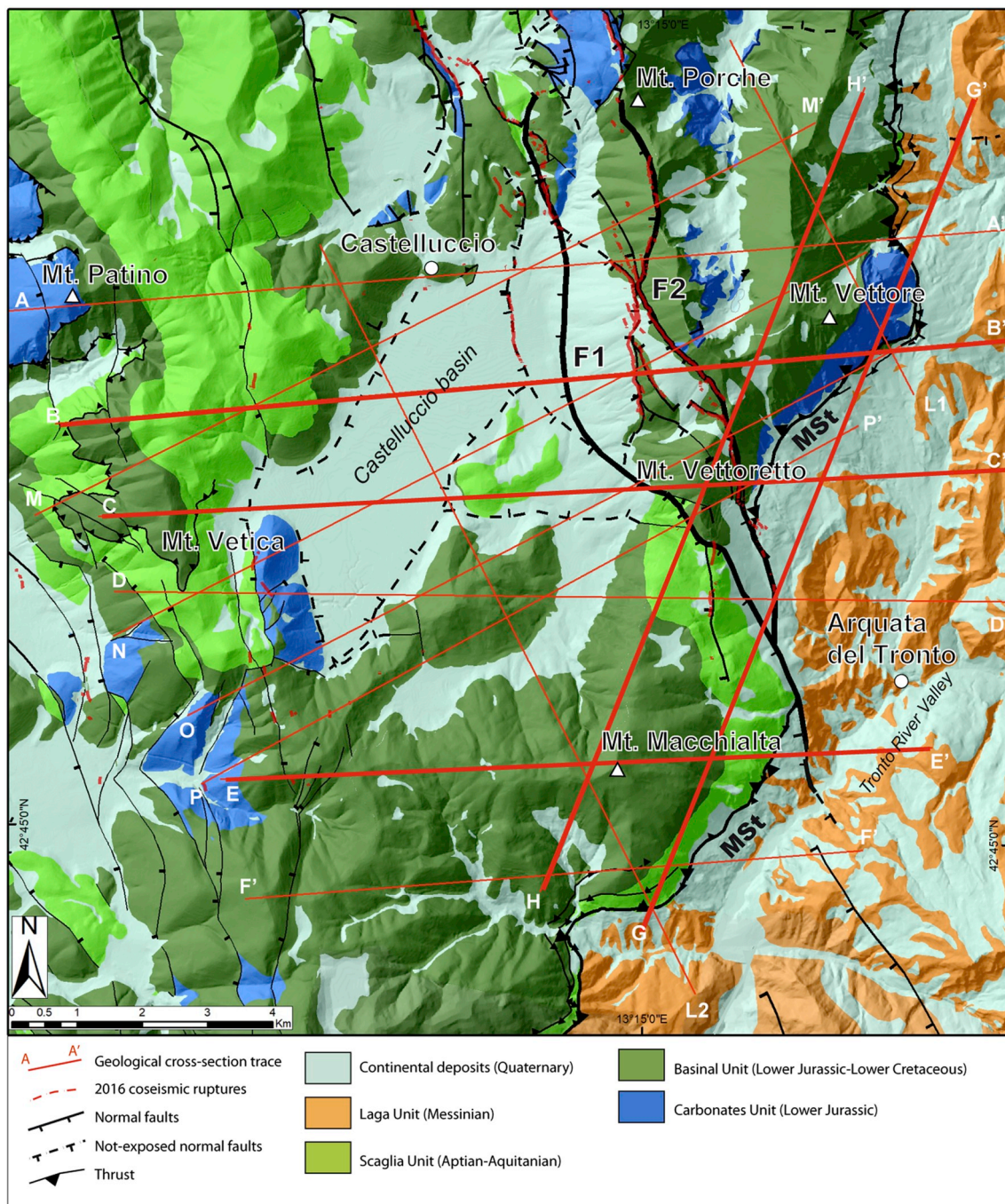


Fig. 3. Simplified geological map and traces of the geological sections produced in this work. The geological map was based on previous works of Centamore et al. (1992) and Pierantoni et al. (2013). The thick red lines are referred to the geological sections shown in Fig. 4. All the sections are in the SM1. The dotted red lines indicate the coseismic surface ruptures on the M. Vettore area and its southward continuation to the Laga siliciclastic Fm. (For interpretation of the references to colour in this figure legend, the reader is referred to the Web version of this article.)

3. Methods

This study is based on the integration of analysis of geological maps and structural survey data to characterize the geometries at depth for the M. Vettore seismogenic fault system (Vf) and its relationships with the MSt. In particular, we focus on the southern termination of the Vf (for an along-strike distance of ca. 10 km), where the maximum geological (long-term) and co-seismic (short-term) displacements, as well as the cross-cutting relations between MSt and Vf, are recorded.

Our 3D geological model of the M. Vettore area is based on the interpolation of 14 geological cross-sections (parallel- and orthogonal-

oriented with respect to the orogenic trend) (Fig. 4 and SM1; traces in Fig. 3), using published geological maps as the base for their construction (Pierantoni et al., 2013; Centamore et al., 1992).

The geological sections and the 3D model were constructed using the 2D and 3D Move software respectively (Midland Valley ©). Once the 3D model was constructed (see SM2), the 3D geometry of the seismogenic Vf, and the isobath contour maps of the MSt and the top of Maiolica Fm. were extrapolated, as described below.

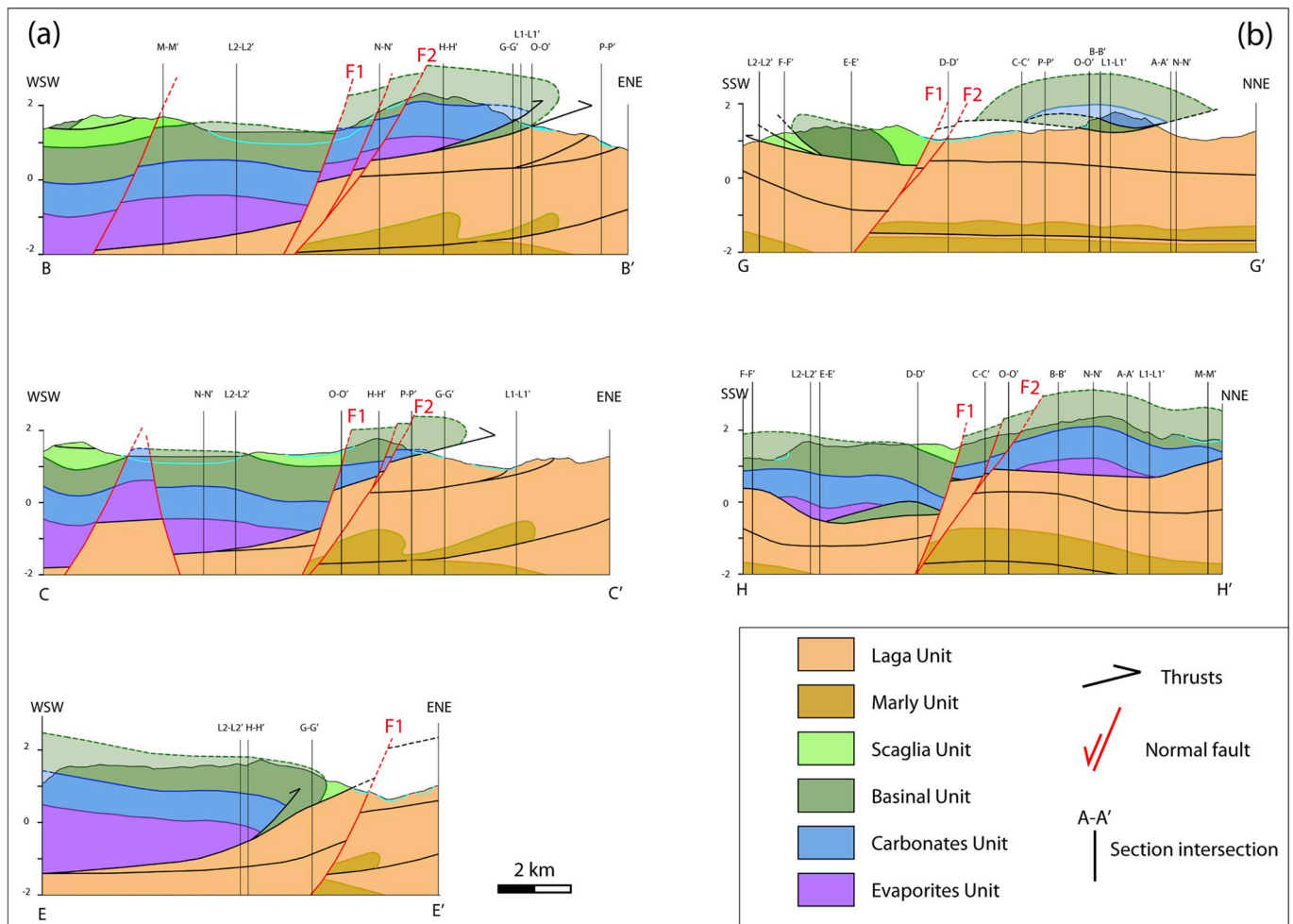


Fig. 4. Three geological cross-sections (a), orthogonally oriented with respect to the arc-shaped compressional structures and slightly oblique to the NNW-SSE striking extensional structures, show the displacement of the M. Sibillini thrust (MSt) by the F1 and F2 belonging to the M. Vettore seisogenic fault system (Vf). The longitudinal (SSW-NNE-oriented) cross sections (b) highlight the along-strike MSt and its displacement controlled by Vf system.

3.1. Geological maps and cross-sections

A new simplified geological map was produced using geological maps available in the literature (Centamore et al., 1992; Pierantoni et al., 2013; Brozzetti et al., 2019), and observations of cross-key locations in the field (see Fig. 3), by means of grouping different geological formations as shown in Fig. 2. The attitudes of the formational boundaries and major faults (Lavecchia et al., 1985; Villani et al., 2018b; Iezzi et al., 2018; Brozzetti et al., 2019), as well as their intersections with the topography, were used to extrapolate the surfaces to depth and onto the multiple geological cross-sections. This technique allowed the reconstruction of the geometries of the tectonic units down to 3000 m depth and also their extrapolation above ground level (Fig. 4). The resolution of our geological map shows several both major and minor structures (i.e. minor faults and formational boundaries), but for our purposes we simplified the geological model, and focused on the relationships between the major faults. For instance, the western side of the M. Vettore is characterised by a synthetic fault splay (SW-dipping), comprised by an arrangement of at least four normal faults. In our sections we did not consider two minor faults producing a small displacement (less than 60 m) compared to the master fault, whose displacement is greater than 1 km. Also, to be consistent with the mainly normal kinematics of coseismic slip vectors recorded along M. Vettore area through geological observations (Iezzi et al., 2018; Villani et al., 2018b), and GPS and SAR interferograms (Cheloni et al., 2017; Scognamiglio et al., 2018), the current model adopts a purely dip-slip extensional

kinematics for the Vf. We traced two main faults associated with the Vf (thick black lines in Fig. 3), characterized by throws of hundred meters.

On the geological map of Fig. 3 we produced: (a) 6 ca. E-W trending geological sections, orthogonal to the fold axes (i.e. parallel to the shortening direction), (b) 4 ENE-WSW trending sections, orthogonal to the major normal faults (i.e. parallel to the extensional axes), (c) 2 NW-SE trending sections parallel to the normal faults, and (d) 2 NNE-SSW trending sections, almost parallel to the strike of MSt (see Fig. 3). The goal was to have multiple constraints on both compressional and extensional structures for constructing a reliable 3D model.

For our sections, we adopted the structural style seen in the field and documented in previous publications that have reconstructed the detailed geometry of the MSt (Lavecchia, 1985) and the M. Vettore anticline (Pierantoni et al., 2013). The errors associated with construction of the cross-sections and throws are variable and difficult to quantify due to the geological complexity of the area and the widespread coverage of recent sediments. Moreover, assumptions are made in the extrapolation below and above ground level of the structures geometry on the basis of the outcrops data and thicknesses of the formations. An important source of potential error is that the stratigraphic configuration of the study area is particularly complex due to important thickness variations related to the Middle-Late Jurassic syn-sedimentary extensional tectonics (Pierantoni et al., 2013). In particular, remarkable thickness variations occur in the succession comprised between the Calcare Massiccio Fm. and the Maiolica Fm. (see Fig. 2), ranging from a minimum of 800 m in the northwestern area to a maximum of 1150 m in

the M. Vettore and southern sectors. Since this variation shows a southeast increase, parallel to the investigated Quaternary faults, it does not affect significantly our estimation of the offset that has been calculated orthogonally with respect these faults. To simplify our geometrical model, we adopted an average thickness for different sectors following the data reported by Pierantoni et al. (2013).

3.2. 3D modeling and contour maps

The geological cross sections were used to create the 3D geological model through two independent structural surfaces: a stratigraphic surface (top Maiolica Fm.) and a tectonic surface (MSt), with the aim of measuring the along-strike throw distribution of the Vf. Two contour maps were obtained for these structural surfaces.

In particular, the 3D geometry of the top Maiolica Fm., which is widely outcropping in the hangingwall of the Vf, was reconstructed using the stratigraphic information reported in the cited maps, as well as in published cross-sections. In the footwall block, the extrapolation of the top Maiolica Fm. is affected by larger errors due to rare or absent outcrops. Taking into account the thickness variation of the Jurassic sequence, we can estimate a maximum error associated with this extrapolation of ca. 180 m.

The geometries and the dip angles applied for the extrapolation of the MSt in the footwall block of the Vf, benefitted of the isobath data reported by Lavecchia et al. (1985). The geometry and the depth of the MSt in the hangingwall of the Vf, less constrained by surface geology data, depends strongly on the adopted structural style. Even if the structural style of Umbria-Marche thrust and fold belt is still matter of debate (e.g. Scisciani et al., 2014; Porreca et al., 2018; Mancinelli et al., 2019), in our sections we adopted a thin-skinned tectonic style with basal decollments within the Evaporites Unit (Bally et al., 1986; Barchi et al., 1998; Sage et al., 1991; Pierantoni et al., 2005, 2013). In detail, the depth of the MSt was inferred using the thickness of the stratigraphic sequence involved in the thrusting and the regional dip of the thrust. The thicknesses of the non-outcropping units (e.g. Triassic Anidriti Burano Fm.) were estimated from well stratigraphy (e.g. Varoni 1; Antrodoco 1; Villadegna 1; see Bally et al., 1986; Barchi et al., 1998 among the others).

The “3D Model Builder” by Move allowed us to reconstruct the stratigraphic surfaces and faults geometry (Fig. 5). The so-called “ordinary Kriging algorithm” was adopted to create the 3D geometry of the

main stratigraphic and structural surfaces.

3.3. Throw distribution

In order to constrain how throw is distributed along-strike of the majors faults, the locations of cut-offs were measured on different stratigraphic-structural surfaces (e.g. Peacock and Sanderson, 1991). In particular, fault throws have been measured using two independent markers (Top of Maiolica Fm. and MSt). These two surfaces are projected onto the faults F1 and F2 to define their along-strike variability of the throw, as well as their aggregate values.

We estimate that the throws derived from our model are associated with errors of less than about 180 m, similar to the errors estimated by other authors (e.g. Iezzi et al., 2018; Brozzetti et al., 2019).

4. Results

4.1. Geological cross-sections

Fig. 4 reports five representative geological cross-sections derived from the 3D model: three ENE-WSW (Fig. 4a) and two NNE-SSW oriented (Fig. 4b) sections. They show the geometrical relationship between active normal faults and pre-existing structures (folds and thrusts). All the other cross-sections are reported in the Supplementary Material (SM1).

The compressional phase was responsible for the origin of the M. Vettore anticline and the MSt. The WSW-ENE oriented sections clearly show the asymmetrical shape of the M. Vettore anticline, characterized by a steep to overturned forelimb involving the Maiolica Fm. and the Scaglia Group (Fig. 4a). In particular, the outcropping part of the anticline in the northern sector is composed predominantly by Early Jurassic Formations (e.g. Corniola Fm. and Calcare Massiccio Fm.) (Sections B–B' and C–C' in Fig. 4a), whereas the southern sector is characterised by widespread exposure of younger formations belonging to the basinal sequence (e.g. Maiolica Fm.) (Section E–E' in Fig. 4a). In particular, in this sector (i.e. in the Vf footwall block) we have observed that the front of the overturned anticline is characterized by the occurrence of Scaglia Bianca Fm. (Scaglia Unit), that is in stratigraphic sequence with the Maiolica Fm. This allows us to exclude the occurrence of a normal fault affecting the overturned Maiolica Fm., as reported by previous geological maps (see Pierantoni et al., 2013). All these units overthrust the

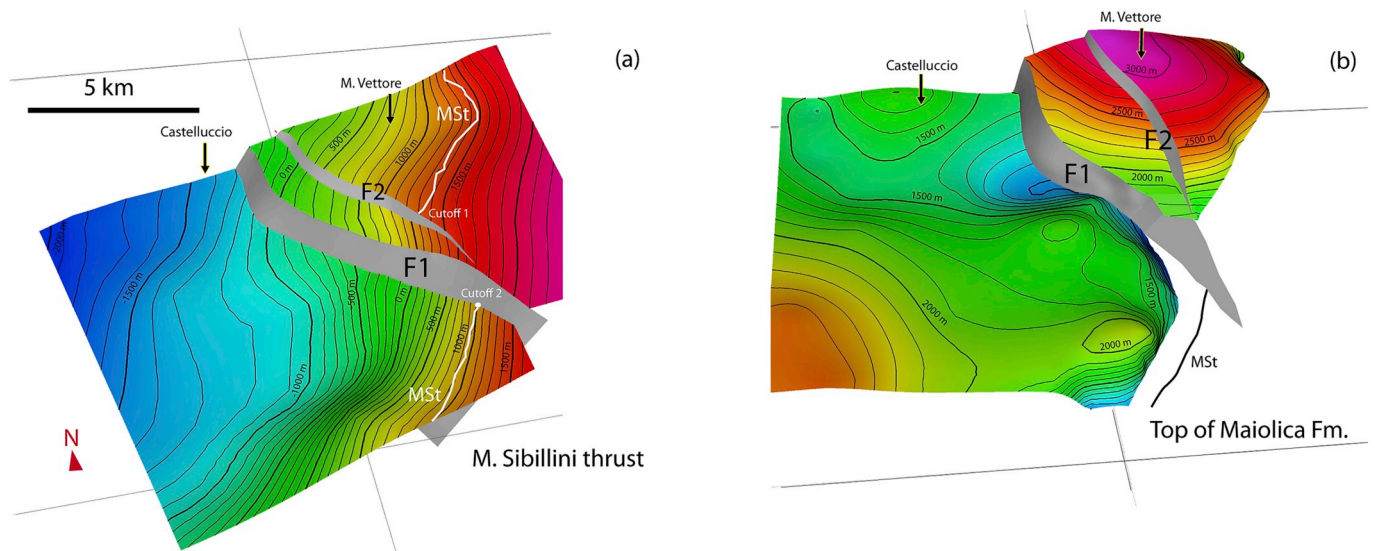


Fig. 5. 3D view of the MSt (a) and the top of Maiolica Fm. (b) surfaces. In (a) the outcropping MSt is reported with a white line, whereas the footwall and hangingwall cutoffs of the MSt are indicated by cutoff 1 and cutoff 2 respectively. In (b) the MSt is reported by a black line. The north is indicated by the red arrow. (For interpretation of the references to colour in this figure legend, the reader is referred to the Web version of this article.)

Laga succession by means of the gently west-southwest dipping (10–20°) MSt (cfr. Lavecchia, 1985; Pierantoni et al., 2013), widely outcropping in the northern and southern sectors of the investigated area.

The subsequent extensional faults cross-cut both the anticline and the MSt. In our geological cross-sections, the Vf is represented by two main high angle WSW-dipping faults, well exposed along the western slope of the M. Vettore (sections B–B', C–C' in Fig. 4a). Fault 1 (F1), is the western fault, that is, the Vf bordering the Castelluccio basin, whilst Fault 2 (F2) is the eastern fault localized on the ridge of the M. Vettore–M. Porche (Fig. 3). Further north and south, these faults coalesce into a single main fault (see Iezzi et al., 2018; Brozzetti et al., 2019). The largest throw occurs across F1 as shown by section C–C' (Fig. 4a). In this area, the F1 juxtaposes the Upper Cretaceous Scaglia Unit (hangingwall) against the Lower Jurassic Corniola Fm. (footwall), with a throw of ca. 1100 m. The throw calculated for F2 is on the order of 200–300 m (sections A–A' to C–C'; Fig. 4a and SM1).

These faults cut and displace the MSt in the subsurface, with significant amounts of throw as shown in the longitudinal sections G–G' and H–H' (Fig. 4b).

4.2. Contour maps

Surface and cross-section data were interpolated to build contour maps of the MSt and the top of the Maiolica Fm., and used to depict the 3D geometry of the structures in the M. Vettore area and their cross-cutting relationships (Figs. 5 and 6).

The contour map in Fig. 6a shows the isobaths of the MSt. Our model shows that the MSt mostly dips W to WNW, apart from the southern sector where it is mainly NW-dipping, consistent with the trace of the thrust at the surface. Regarding the dip angles, in the northern sector, a dip of ca. 22°–26° is obtained for the shallower part, gradually decreasing at depth to 8–12°; in contrast, in the southern part we obtained higher dip values for the frontal part of the thrust (30–35°), probably due to a lateral ramp geometry.

The MSt surface is cut by the main NNW-SSE trending F1 and F2 faults, belonging to the Vf system (Fig. 6a), which exhibit predominant dip slip kinematics and merge south-east of M. Vettore (Fig. 3). The MSt surface is therefore divided in three main blocks: from east to west, the outer block located under the M. Vettore–Vettore area, in the

footwall of the Vf system; the intermediate block, delimited by F1 and F2 faults, and the western block, under the Castelluccio basin, which experienced the aggregate effect of tectonic subsidence due to both faults.

The contour map of the top Maiolica Fm (Fig. 6b). shows a more complex geometry. In particular, the top Maiolica Fm gains its maximum culmination close to the M. Vettore peak, with an inferred structural elevation of ca. 2900 m, and a minimum elevation of 1100 m above sea level, in correspondence with the depocenter of the Castelluccio basin; therefore an elevation change of ca. 1800 m is estimated across both F1 and F2. Iezzi et al. (2018) suggest that this localized area of high offset is related to an along-strike bend in the fault system. The south-eastern part of the Maiolica surface is characterized by a steep geometry corresponding to the overturned forelimb, with a gently NNW plunging culmination that is likely to be related to the occurrence of the steep lateral ramp of the MSt.

4.3. Throw distribution

The cutoffs of the reconstructed top Maiolica and MSt surfaces in the Vf hangingwall and footwall (SM3 in Supplementary material) have been used to construct the along-strike throw distribution of the Vf. The along-strike variation of throw of the two surfaces, across both F1 and F2, along with the cumulative throw, is shown in Fig. 7. The average value of throw has been calculated using both structural surfaces in the hangingwall of the MSt in the northern sector (from 0 to 5.5 km progressive distance in Fig. 7), where the Maiolica Fm. crops out. In the southern sector of the MSt footwall (from 5.5 to 9 km in Fig. 7), the throw values were estimated using only the displacement of the MSt.

In the first 5.5 km of the studied Vf, the top Maiolica and the MSt have similar throw variation. Here an average value has been calculated taking into account both the surfaces (dashed black line in Fig. 7). The average throw for both the faults is characterized by an almost flat geometry, with a subtle increase towards the south. In particular, the throw along F1 increases from ca. 900 m up to maximum of 1000 m (cross-section B–B'). The throw along F2 ranges from ca. 200 m (section M–M') to a maximum of 300 m (section C–C'). In the southern sector, starting from the distance of 5.5 km, we note a marked increase of the throw along F1 corresponding to a decrease along F2, with the latter will

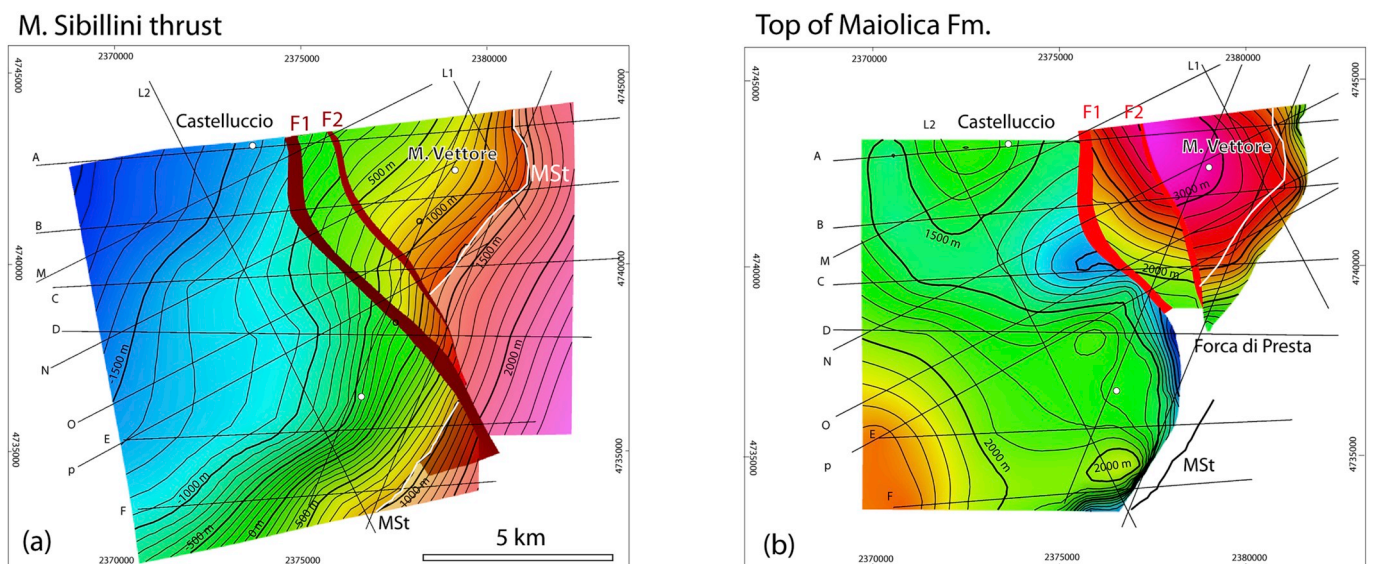


Fig. 6. Contour structural maps of the MSt (a) and the top of Maiolica Fm. (b). The maps have been constrained by the geological cross-sections (thin black lines) and outcropping stratigraphic and tectonic contacts (geological map by Pierantoni et al., 2013). (a) Contour map of the MSt cut by the seismogenic Vf system represented by F1 and F2. The white curved lines are the surface evidence of the thrust, which constrains the model. The eastern sector of the MSt surface is extrapolated over the topography. (b) Contour map of the top Maiolica Fm. surface. The black curve represents the outcrop traces of the MSt. The top Maiolica Fm. in the Vf footwall block was extrapolated using the average thickness of the Basinal Unit. See the text for further details.

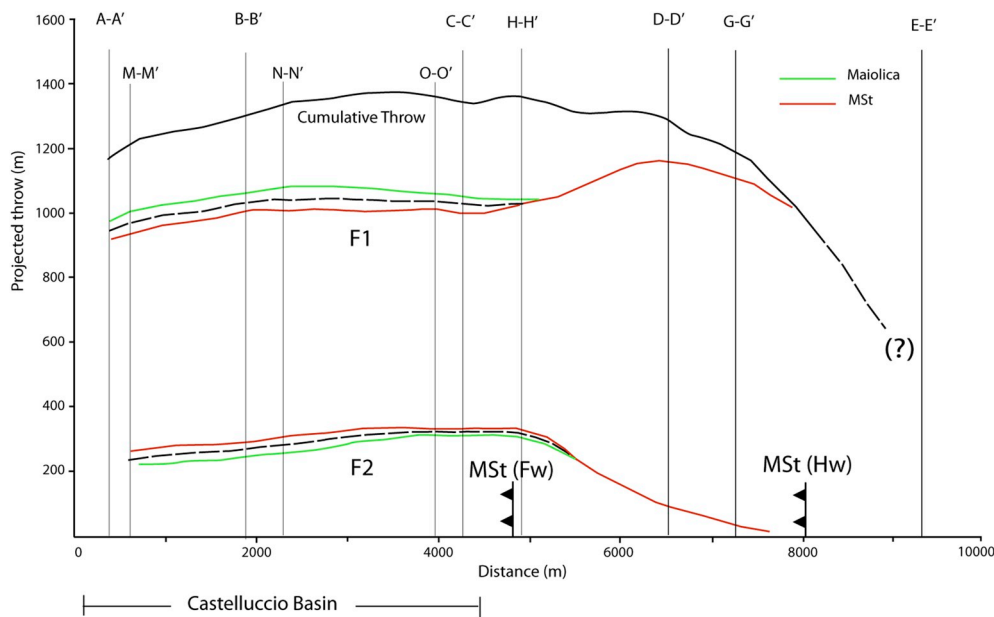


Fig. 7. Throw distribution along the two faults (F1 and F2) of the M. Vettore area. The green line is referred to the top of Maiolica Fm., whereas the red line to the MSt. The average throw calculated using these two reference surfaces is reported as dashed lines only in the northern sector. The cumulative throw is given by the sum of F1 and F2 and is indicated by black continuous line. The southern termination of the fault is not constrained by geological cross-sections. MSt (Fw): the MSt cutoff in the footwall of the Vf; MSt (Hw): the MSt cutoff in the hangingwall of the Vf. (For interpretation of the references to colour in this figure legend, the reader is referred to the Web version of this article.)

decreasing to a throw of zero where it coalesces with F1 (Fig. 7).

The cumulative throw across the two faults depicts a bow-shaped trend with the maximum throw of ca. 1380 m between sections B-B' and C-C' (Fig. 7), in correspondence of the M. Vettoreto segment. This is also the area where the maximum co-seismic throw was recorded after the Mw 6.5 mainshock (Iezzi et al., 2018; Villani et al., 2018a; Brozzetti et al., 2019).

Towards the south, the cumulative throw decreases, reaching a value of ca. 600 m as estimated along the E-E' cross-section within the Laga Fm (Fig. 7). The possible continuation of the Vf to the south is discussed below.

5. Discussion

The 3D reconstruction of the geometry and kinematics of the NNW-SSE-trending Vf and the arcuate pre-existing MSt reveals a clear cross-cutting relationship, where the well-exposed Vf cuts and displaces the MSt. In this section, we first discuss the reconstruction of the along-strike throw variation of Vf and its continuation to the south-east with respect to the MSt. Secondly, we analyse how the lithology may have controlled the distribution and the expression of the surface co-seismic ruptures. In the last section we compare the net geological and 2016–2017 coseismic throw distributions, to discuss if the latter is representative of the long-term expression of the active fault.

5.1. Throw gradient and fault propagation

Most published geological maps show that the southern tip of the surface trace of the Vf is located in the vicinity of the MSt, and is organized in splays that appear to curve to the thrust trend (e.g. Pizzi and Galadini, 2009; Bonini et al., 2016). This has been interpreted in different ways, such as a steep displacement gradient near the tip in vicinity of the thrust, but with the normal fault displacing the thrust, or the surface expression of a normal fault that has the geometry of a splay that detaches onto the thrust surface.

However, in contrast to the above interpretations, in our 3D reconstruction the Vf cannot be a splay of the thrust that was reactivated in an extensional regime. In fact, the Vf clearly cuts the MSt and continues within the footwall of the MSt, i.e. within the Laga Fm. This hypothesis is supported by the location of the maximum throw of ca. 1380 m, which is within the range of throws across major active faults in the Apennines of

ca. 1–2 km (Roberts and Michetti, 2004), yet is located within only 1–3 km of the mapped intersection of the MSt, in the M. Vettoreto area. If the Vf has a typical tip displacement gradient, it is likely that the fault continues for a number of kilometres to the SE, beyond the point of intersection, otherwise the fault would have a very unusual, extremely high asymmetric displacement profile. For example, in the central Apennines, throw/length (d/L) ratios on faults are in the range of 0.035–0.083 (Pizzi et al., 2002; Roberts and Michetti, 2004), and the faults tend to have symmetrical displacement profiles (see Fig. 8 of Roberts and Michetti, 2004), so these observations set typical values for tip gradients. For example, for faults in the dataset compiled by Roberts and Michetti (2004), the points of maximum throw occur at distances of 21–31% of the total fault lengths away from mapped fault tips (Supplementary material SM4a); the preferred interpretation in this paper is close to this, having a value of 13%. However, if the Vf terminated at the MSt near either M. Vettoreto or M. Macchialta (see Fig. 3), the implied value would be between 1 and 6% (Supplementary material SM4b), which we feel is not plausible. Thus, for the throw to decrease to zero exactly at the MSt it would imply an implausible, extremely high tip gradient that we do not recognize on other faults in the Apennines.

Moreover, the variation of slip-directions can help to define the fault lengths because they vary with throw and distance (Ma and Kuszniir, 1995; Roberts, 1996; Michetti et al., 2000; Roberts and Ganas, 2000; Hampel et al., 2013). Throw gradients produce stretching of the ground surface along strike so slip-directions converge towards the hanging-wall to accommodate the stretching. Fault lengths should therefore be reflected in the length scale of the converging patterns of fault slip. For the Vf, there exists a wealth of published data on the slip-directions distributions (e.g. Ferrario and Livio, 2018; Iezzi et al., 2018; Perouse et al., 2018; Villani et al., 2018b; Brozzetti et al., 2019). In particular, values for the slip vector azimuth measured by different authors on the fault planes after the August 24th and October 30th 2016 events (Amatrice and Norcia earthquakes respectively) range between N210° and N270°, with an average of N251° (Iezzi et al., 2018; Villani et al., 2018a), which is perpendicular to the overall fault strike and not influenced by the slope dip direction. None of the published data show any convergence of the slip directions in proximity with the supposed fault termination (i.e. the intersection with MSt) (Supplementary material SM4c), suggesting that instead, the tip is located further to the SE in the poorly-exposed area of the Laga Fm.

Taken together, the data regarding the throw gradient and slip-

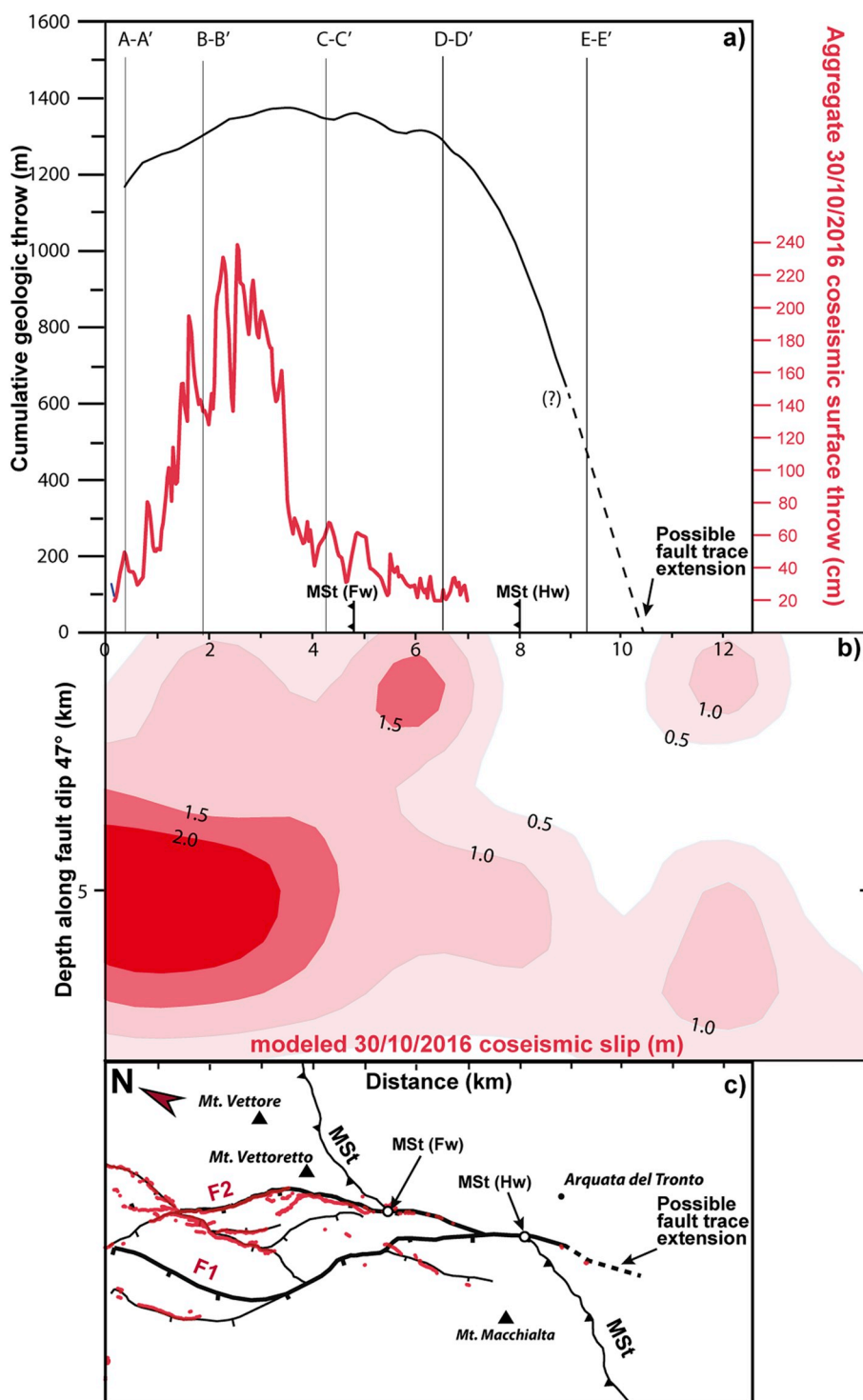


Fig. 8. Comparison between geological and 2016–2017 coseismic expressions. (a) Along-strike distribution curve of both cumulative net geologic and the October 30th Mw 6.5 coseismic surface rupture (Villani et al., 2018a) throws. Locations of MSt cutoff are reported; (b) along-strike distribution of the Mw 6.5 slip on fault plane at depth modeled from strong motion data (Scognamiglio et al., 2018); (c) Sketch of the southern pattern of the VBFS and its relationship with the MSt. The Mw 6.5 coseismic surface rupture is drawn in red (Villani et al., 2018a). Thick black lines indicate the F1 and F2 fault splays utilized for the geologic 3D model. MSt cutoff and possible Vf southern extension derived from the model are reported. (For interpretation of the references to colour in this figure legend, the reader is referred to the Web version of this article.)

directions suggest therefore that the fault must continue toward the south, in the MSt footwall, within the siliciclastic Laga Fm. We therefore have estimated the southern propagation of the Vf using typical throw gradient values of active normal faults of the central Apennines as measured by Roberts and Michetti (2004). The authors found an average d_{max}/L ratio of ca. 0.13 for these faults (where d_{max} is the maximum throw and L is the distance between the point of d_{max} and the nearest fault tip), whereas the highest ratio is of ca. 0.21. If we apply the highest ratio to the Vf, then a value of ca. 6.7 km represents the minimum distance of the SE fault termination with respect to the M. Vettoretto area (i.e. the location of d_{max}) (Fig. 8a). Thus, this implies that estimated tip

point of the fault ought to be located beyond the intersection with the MSt. Furthermore, the typical tip gradient values we have used are consistent with the faults that we have traced in the geological map of Fig. 3 and also in agreement with the fault tips identified by Iezzi et al. (2018) and the fault continuation of Brozzetti et al. (2019).

5.2. Lithological control on the surface co-seismic ruptures

We suggest lithology may play a role in controlling the morphological expression of the normal faulting and this may help to explain why debate surrounds the nature of relationship between the Vf and the MSt.

The surface ruptures to the August 24th (Mw 6.0) and the October 30th (Mw 6.5) 2016 earthquakes are far more spectacularly and continuously exposed in the MSt hangingwall, where carbonate rocks crop out at the surface, than in its footwall, characterized by outcropping siliciclastic rocks of the Laga Fm. (Livio et al., 2016; Pucci et al., 2017; Ferrario and Livio, 2018; Perouse et al., 2018; Villani et al., 2018a; Brozzetti et al., 2019). This difference might be due to a combination of earthquake location near the rupture fault tip and the occurrence of a cover of colluvium above the flysch lithology that hampers the rupture propagation at surface.

Also over a longer time scale (i.e. Quaternary), normal faults cutting carbonate rocks (e.g. M. Vettore, M. Bove ruptures Calamita and Pizzi, 1992; Calamita et al., 1992; Calamita et al., 1994b) are characterized by clearer morphotectonic evidence compared to similar faults cutting siliciclastic rocks. Boncio et al. (2004), for example, describing the Gorzano fault (Gf), reconstruct long-term total net displacement in excess of 2000 m, with limited exposure of clear fault surfaces restricted to only the central part of the fault where marly limestones are exposed near the base of the Laga Fm.

A similar morphological contrast characterizes other Quaternary faults of the Umbria-Marche region, like the Gubbio fault (Collettini et al., 2003; Pucci et al., 2003): the northern part of the fault, where the footwall consists of carbonate rocks, is characterized by well-preserved fault surfaces and prominent fault scarps, which lack in the southern portion of the fault, where Miocene turbidites crop out at the fault footwall. In this case, the southward decrease of the long-term throw, observed in the seismic profiles, possibly contributes to the different morphological expression of the fault (Pucci et al., 2003; Mirabella et al., 2004).

In part, the different morphology of the long-term, Quaternary faults might be explained by the different erodibility of the footwall rocks, which promote a better preservation of the fault scarps in the harder carbonates with respect to the softer turbidites. However, the differential erodibility cannot be invoked to explain the discontinuity or absence of surface ruptures, since they form quasi-instantaneously during the 2016 mainshocks (Pucci et al., 2017; Wilkinson et al., 2017; Villani et al., 2018a). In this case the different expression of the coseismic ruptures affecting the hangingwall and footwall of the MSt can be explained by the combined effect of: i) diminishing fault displacement towards the southern termination of the fault and also ii) a less effective rupture propagation, from the deep seismic source up to its surface expression, possibly driven by lithological (= mechanical) control. The lithological control in promoting inelastic deformation is quite obvious: less competent rocks are commonly associated with a more distributed deformation; this is likely to be true for surface ruptures, as recently discussed for the surface faulting of the 2016–2017 seismic sequence by Carminati et al. (2019). In particular, the thickness of the overburden of loose sedimentary cover influences the surface expression of faulting, as observed in several surface faulting worldwide (Milliner et al., 2015; Teran et al., 2015; Zinke et al., 2014). Similarly to the Central Italy 2016 surface ruptures, also the 1980 Irpinia Mw 6.9 earthquake produced surface ruptures were mainly affecting the carbonate sequences of the Southern Apennines. Also in this case, the Irpinia fault did not show any clear evidence of surface rupture where it affects soft turbidites units at the Sele Valley (Pantosti and Valensise, 1990).

Also, accurate hypocentral locations of seismic events, including aftershocks, show that in the Umbria-Marche extensional belt the seismicity distribution is affected by the mechanical stratigraphy of the sedimentary cover, providing further evidence of the inelastic behavior of the Central Italy turbidites with respect to the underlying carbonates. For example in the 2016–2017 seismic sequences, the longitudinal sections published by Chiaraluce et al. (2017) (Fig. 3, sections 2b and 2c) and by Improta et al. (2019) (sections of Fig. 3) show that the seismicity shallower than 4 km abruptly disappears in the part of the section crossing the Laga deposits, between the MSt and the Gran Sasso thrust. A similar behavior has also been observed for the Gualdo Tadino 1998

sequence (Ciaccio et al., 2005), as well as for the Pietralunga 2012 sequence (Latorre et al., 2016): in both cases the seismicity seems to be distributed only in the carbonate and evaporite dominated lithologies and does not affect the uppermost part of the sedimentary cover, consisting of the Marnoso-Arenacea turbidites.

We are conscious that this is a relevant and critical topic, which is worthy of further investigation using a specifically dedicated approach aimed at describing the effects of the lithology on the deformation pattern (e.g. Peacock and Sanderson, 1992; Giorgetti et al., 2016). However, our main point is that it is likely that the debate about the exact relationship between the Vf and the MSt has been exacerbated by both the presence of less competent rocks and both coseismic and longer-term displacements decreasing towards the fault tip.

5.3. Comparison between net geological and 2016–2017 coseismic displacements

The coseismic expression of the 2016–2017 seismic sequence affecting the study region presents two main analogies with the long-term picture derived by our 3D geologic model: 1) the shape of the along-strike distribution curve of Vf displacements; 2) the Vf offset and displacement of the pre-existing MSt.

Fig. 8 shows the comparison between the along-strike distributions of the net geological (black line) and the Norcia earthquake (October 30th Mw 6.5) coseismic surface rupture (red line from Villani et al., 2018a), the slip on fault plane at depth (modeled from strong motion data, from Scognamiglio et al., 2018), and their locations with respect to the southern part of the Vf and the MSt.

Both net geological and coseismic displacements reach the maximum values where they involve carbonate rocks and in coincidence of the largest relief (Pizzi et al., 2017; Iezzi et al., 2018). As a consequence, the Maiolica surface shows the lowest elevation in correspondence of the eastern sector of the Castelluccio basin, where the maximum aggregate coseismic throw was observed at the surface (Iezzi et al., 2018; Villani et al., 2018b; Brozzetti et al., 2019). The minimum elevation of the Maiolica surface at the F1 hangingwall corresponds also to the maximum coseismic subsidence indicated by geodetic data for both the August 24th and October 30th 2016 earthquakes (Lavecchia et al., 2016; Cheloni et al., 2017; Xu et al., 2017; Walters et al., 2018; Tung and Masterlark, 2018).

The coseismic surface rupture throw, most of which occurred on the F2 splay, decreases and extends south of the MSt footwall cutoff, where the fault affects loose landslide and siliciclastic deposits, while the net geological throw remains high (Fig. 8a). Moreover, the October 30th slip on fault plane at depth (Scognamiglio et al., 2018), although decreasing, appears to clearly extend well beyond (4–5 km) both the MSt (Fw) and MSt (Hw) cutoffs, with patches of values > 1.0 m (Fig. 8b and c). The resulting geologic model of Vf crosscutting the MSt is also in agreement with slip distribution modeled from geodetic and strong motion data of the August 24th Mw 6.0 Amatrice earthquake (Pizzi et al., 2017; Cirella et al., 2018). Thus, our overall point is that it appears that the long-term slip and coseismic slip in 2016 both continued beyond the point of intersection with MSt.

6. Conclusions

The 2016–2017 Central Italy earthquakes represent a unique well-observed geological example that sheds light on the spatio-temporal evolution of seismic sequences cross-cutting pre-existing tectonic discontinuities. In order to provide constraints onto the relationships between seismogenic faults (the Vettore fault, Vf) and inherited compressional structures (the M. Sibillini thrust, MSt), we have reconstructed a 3D geological model of the first-order structural elements in this seismically area of the Apennines. This was possible thanks to a grid of 14 geological cross-sections drawn across an updated geological map of the area. Having a 3D model, independent from any a priori structural

interpretation, helped us to discriminate in an area of complex structures between various potential interpretations based largely on field data and 2D geological sections.

The results of this work have clearly demonstrated that the seismogenic WSW-dipping Vf displaces the arcuate-shaped MSt with a vertical offset of more than 800 m. The Vf cuts the MSt and continues within the Messinian Laga domain, for at least 6 km from the location of the maximum throw given a typical throw gradient for normal faults of the Apennines. Throw variations along the Vf increase from its northern sector to its central part, depicting a rough bow-shaped curve that shows a maximum of almost 1400 m near M. Vettoreto, in proximity of the intersection with the MSt. Southward, the cumulative throw values decrease markedly reaching about 600 m within the Laga Fm. All the evidence presented and discussed in this study, such as the 3D geometrical model, the throw gradient, the long- and short-term behavior of the Vf, the co-seismic ruptures and their response to different lithologies, converge to the same scenario including a cross-cut relations between Vf and the MSt, and rejecting the hypothesis that the thrust was reactivated during the last seismic sequence.

The significance of this observation goes beyond that of the local geology of Central Italy. We point out that identifying the lateral tips of normal faults is difficult because the point where the displacement decreases to zero may be challenging to identify if the fault is difficult to resolve in less-competent rock, yet defining the tip is critical to define the maximum expected magnitude. For example, databases detailing scaling relationships between maximum displacement, maximum magnitude and fault length are only as good as the data they contain pertaining to the locations of rupture tips (e.g. Wells and Coppersmith, 1994; Leonard et al., 2010). We stress the need for detailed mapping and 3D reconstruction near fault tips, as we have demonstrated in this paper.

Ultimately, this case study illustrates the importance of the geological cross-sections to construct a reliable 3D geological model and its value to constrain the sub-surface geometry of tectonic structures also for studies of earthquakes. This kind of model may represent the geometrical “box” to be filled by the data coming from different approaches (e.g. seismology, geodesy, well-stratigraphy) for next studies of important seismic sequences such as that of 2016–2017 Central Italy.

Declaration of competing interest

We wish to confirm that there are no known conflicts of interest associated with this publication and there has been no significant financial support for this work that could have influenced its outcome.

CRediT authorship contribution statement

Massimiliano Porreca: Conceptualization, Methodology, Investigation, Writing - original draft, Writing - review & editing. **Andrea Fabbrizzi:** Methodology, Data curation, Visualization. **Salvatore Azzaro:** Data curation, Investigation. **Stefano Pucci:** Validation, Resources, Writing - original draft. **Pietro Paolo Pierantoni:** Resources, Data curation. **Claudia Giorgetti:** Investigation, Data curation. **Gerald Roberts:** Conceptualization, Formal analysis, Writing - review & editing, Visualization. **Massimiliano Rinaldo Barchi:** Conceptualization, Supervision, Writing - review & editing.

Acknowledgements

We are particularly grateful to the reviewers and the Editor for their constructive and stimulating discussion. The suggestions of the reviewers have allowed to strongly improve our paper. The activities of this work were supported by the research grant funded by the Fondazione Cassa di Risparmio di Perugia (Italy) entitled “Studi geologici e geofisici di superficie e di sottosuolo per la caratterizzazione 3D delle faglie sismogeniche del territorio umbro: un contributo per la definizione della pericolosità sismica della regione” (Grant n. 2018.0416,

Resp. M. R. Barchi) and by the research grant supported by Dipartimento di Fisica e Geologia, Università di Perugia (Fondi Ricerca di Base 2017; Resp. M. Porreca).

The database encompassing the geological maps and the geological cross-sections were produced with the software 2D and 3D MOVE 2017, © Midland Valley Exploration Ltd.

Appendix A. Supplementary data

Supplementary data to this article can be found online at <https://doi.org/10.1016/j.jsg.2019.103938>.

References

- Albano, M., Saroli, M., Moro, M., Falcucci, E., Gori, S., Stramondo, S., Galadini, F., Barba, S., 2016. Minor shallow gravitational component on the Mt. Vettore surface ruptures related to MW 6, 2016 Amatrice earthquake. *Ann. Geophys.* 59 (5) <https://doi.org/10.4401/ag-7299>.
- Alvarez, W., 1989. Evolution of the Monte Nerone seamount in the Umbria-Marche Apennines. 2. Tectonic control of the seamount basin transition. *Boll. Soc. Geol. It.* 108, 23–39.
- Bally, A.W., Burbi, L., Cooper, J.C., Ghelardoni, R., 1986. Balanced sections and seismic reflection profiles across the Central Apennines. *Mem. Soc. Geol. Ital.* 35, 257–310.
- Barchi, M.R., DeFeyter, A., Magnani, B., Minelli, G., Piali, G., Sotera, B., 1998. The structural style of the Umbria–Marche fold and thrust belt. *Mem. Soc. Geol. Ital.* 52, 557–578.
- Barchi, M.R., 2010. The Neogene-Quaternary evolution of the Northern Apennines: crustal structure, style of deformation and seismicity. *J. Virtual Explor.* <https://doi.org/10.3809/jvirtex.2010.00220>.
- Boccaletti, M., Coli, M., 1982. Carta Strutturale dell'Appennino Settentrionale. Progetto Finalizzato Geodinamica, Pubblicazione N. 429. SELCA, Firenze.
- Boccaletti, G., Ferrari, R., Adcroft, A., Ferreira, D., Marshall, J., 2005. The vertical structure of ocean heat transport. *Geophys. Res. Lett.* 32 (L10603) <https://doi.org/10.1029/2005GL022474>.
- Boncio, P., Lavecchia, G., Milana, G., Rozzi, B., 2004. Seismogenesis in Central Apennines, Italy: an integrated analysis of minor earthquake sequences and structural data in the Amatrice-Campotosto area. *Ann. Geophys.* 47 (6), 1723–1742.
- Bonini, L., Maesano, F.E., Basili, R., Burrato, P., Carafa, M.M.C., Fracassi, U., Kastelic, V., Tarabusi, G., Tiberti, M.M., Vannoli, P., Valensise, G., 2016. Imaging the tectonic framework of the 24 August 2016, Amatrice (central Italy) earthquake sequence: new roles for old players? *Ann. Geophys.* 59 (5) <https://doi.org/10.4401/ag-7229>.
- Brozzetti, F., Lavecchia, G., 1994. Seismicity and related extensional stress field: the case of the Norcia Seismic Zone (Central Italy). *Ann. Tect.* VIII (1), 36–57.
- Brozzetti, F., Boncio, P., Cirillo, D., Ferrarini, F., de Nardis, R., Testa, A., Liberi, F., Lavecchia, G., 2019. High resolution field mapping and analysis of the August - October 2016 coseismic surface faulting (Central Italy Earthquakes): slip distribution, parameterization and comparison with global earthquakes. *Tectonics* 38, 417–439. <https://doi.org/10.1029/2018tc005305>.
- Calamita, F., Pizzi, A., 1992. Tettonica quaternaria nella dorsale appenninica umbro-marchigiana e bacini intrappenninici associati. *Studi Geol. Camerti* 17–25. <https://doi.org/10.15165/studgeocam-1186>. Spec. 1992/1.
- Calamita, F., Pizzi, A., Roscioni, M., 1992. I fasci di faglie recenti ed attive di M. Vettore – M. Bove e di M. Castello – M. Cardosa (appennino Umbro-Marchigiano). *Studi Geol. Camerti* 81–95. <https://doi.org/10.15165/studgeocam-1198>. Spec. 1992/1.
- Calamita, F., Cello, G., Deiana, G., 1994a. Structural styles, chronology rates of deformation, and time-space relationships in the Umbria-Marche thrust system (central Apennines, Italy). *Tectonics* 13 (4), 873–881. <https://doi.org/10.1029/94TC00276>.
- Calamita, F., Coltorti, M., Farabollini, P., Pizzi, A., 1994b. Le faglie normali quaternarie nella Dorsale appenninica umbro-marchigiana. Proposta di un modello di tettonica d'inversione. *Studi Geol. Camerti* 211–225. <https://doi.org/10.15165/studgeocam-1164>. Spec. 1994/1.
- Calamita, F., Coltorti, M., Piccinini, D., Pierantoni, P.P., Pizzi, A., Ripepe, M., Scisciani, V., Turco, E., 2000. Quaternary faults and seismicity in the umbro-marchean apennines (Central Italy): evidence from the 1997 colfiorito earthquake. *J. Geodyn.* 29 (5–5), 245–264. [https://doi.org/10.1016/S0264-3707\(99\)00054-X](https://doi.org/10.1016/S0264-3707(99)00054-X).
- Calamita, F., Paltrinieri, W., Pelorosso, M., Scisciani, V., Tavarnelli, E., 2003. Inherited Mesozoic architecture of the Adria continental palaeomargin in the neogene central apennines orogenic system, Italy. *Boll. Soc. Geol. Ital.* 122 (2), 307–318.
- Carminati, E., Doglioni, C., 2012. Alps vs. Apennines: the paradigm of a tectonically asymmetric Earth. *Earth Sci. Rev.* 112 (1–2), 67–96. <https://doi.org/10.1016/j.earscirev.2012.02.004>.
- Carminati, E., Bignami, C., Doglioni, C., Smeraglia, L., 2019. Lithological control on multiple surface ruptures during the 2016–2017 Amatrice-Norcia seismic sequence. *J. Geodyn.* 101676. <https://doi.org/10.1016/j.jjog.2019.101676>.
- Cavinato, G.P., De Celles, P.G., 1999. Extensional basins in the tectonically bimodal Central Apennines fold-thrust belt, Italy: response to corner flow above a subducting slab in retrograde motion. *Geology* 27 (10), 955–958. [https://doi.org/10.1130/0091-7613\(1999\)027<0955:EBITTB>2.3.CO;2](https://doi.org/10.1130/0091-7613(1999)027<0955:EBITTB>2.3.CO;2).
- Centamore, E., Deiana, G., Micarelli, A., Potetti, M., 1986. Il trias-paleogene delle marche. In: Centamore, E., Deiana, G. (Eds.), *Studi Geologici Camerti, Special Volume La Geologia Delle Marche*, pp. 9–27.

- Centamore, E., Adamoli, L., Berti, D., Bigi, G., Bigi, S., Casnedi, R., Cantalamessa, R., Fumanti, G., Morelli, F., Micarelli, C., Ridolfi, A., Salvucci, M., 1992. Carta geologica dei bacini della Laga e del Cellino e dei rilievi carbonatici circostanti. In: Studi Geologici Camerti, Vol. Spec. Università degli Studi, Dipartimento di Scienze della Terra. SELCA, Firenze.
- Cheloni, D., De Novellis, V., Albano, M., Antonoli, A., Anzidei, M., Atzori, S., Avallone, A., Bignami, C., Bonano, M., Calcaterra, S., Castaldo, R., Casu, F., Cecere, G., De Luca, C., Devoti, R., Di Bucci, D., Esposito, A., Galvani, A., Gambino, P., Giuliani, R., Lanari, R., Manunta, M., Manzo, M., Mattone, M., Montuori, A., Pepe, A., Pepe, S., Pezzo, G., Pietrantonio, G., Polcari, M., Riguzzi, F., Salvi, S., Sepe, V., Serrapelloni, E., Solaro, G., Stramondo, S., Tizzani, P., Tolomei, C., Trasatti, E., Valerio, E., Zinno, I., Doglioni, C., 2017. Geodetic model of the 2016 Central Italy earthquake sequence inferred from InSAR and GPS data. *Geophys. Res. Lett.* 44, 6778–6787. <https://doi.org/10.1002/2017GL073580>.
- Chiaraluce, L., Di Stefano, R., Tinti, E., Scognamiglio, L., Michele, M., Casarotti, E., Cattaneo, M., De Gori, P., Chiarabba, C., Monachesi, G., Lombardi, A., Valoroso, L., Latorre, D., Marzorati, S., 2017. The 2016 Central Italy seismic sequence: a first look at the mainshocks, aftershocks, and source models. *Seismol. Res. Lett.* 88 (3), 757–771. <https://doi.org/10.1785/0220160221>.
- Ciaccio, M.G., Barchi, M.R., Chiarabba, C., Mirabella, F., Stucchi, E., 2005. Seismological, geological and geophysical constraints for the Gualdo Tadino fault, Umbria–Marche apennines (Central Italy). *Tectonophysics* 406 (3–4), 233–247. <https://doi.org/10.1016/j.tecto.2005.05.027>.
- Cirella, A., Pezzo, G., Piatanesi, A., 2018. Rupture kinematics and structural-rheological control of the 2016 Mw6.1 Amatrice (Central Italy) earthquake from joint inversion of seismic and geodetic data. *Geophys. Res. Lett.* 45 (12), 302–312. <https://doi.org/10.1029/2018GL080894>, 311.
- Civico, R., Pucci, S., Villani, F., Pizzimenti, L., De Martini, P.M., Nappi, R., the Open EMERGE Working Group, 2018. Surface ruptures following the 30 October 2016 Mw 6.5 Norcia earthquake, central Italy. *J. Maps* 14 (2), 151–160. <https://doi.org/10.1080/17445647.2018.1441756>.
- Colacicchi, R., Passeri, L., Piali, G., 1970. Nuovi dati sul Giurese Umbro-Marchigiano ed ipotesi per un suo inquadramento regionale. *Mem. Soc. Geol. It.* 9 (4), 839–874.
- Collettini, C., Barchi, M.R., Chiaraluce, L., Mirabella, F., Pucci, S., 2003. The Gubbio fault: can different methods give pictures of the same object? *J. Geodyn.* 36 (1–2), 51–66. [https://doi.org/10.1016/S0264-3707\(03\)00038-3](https://doi.org/10.1016/S0264-3707(03)00038-3).
- Collettini, C., Chiaraluce, L., Pucci, S., Barchi, M.R., Cocco, M., 2005. Looking at fault reactivation matching structural geology and seismological data. *J. Struct. Geol.* 27 (5), 937–942.
- Coltorti, M., Farabolini, P., 1995. Quaternary evolution of the “Castelluccio di Norcia” basin (Umbro-Marchean apennines, central Italy). *Il Quat.* 8 (1), 149–166.
- Cosentino, D., Cipollari, P., Marsili, P., Scrocca, D., 2010. Geology of the central apennines: a regional review. *J. Virtual Explor. umc* 36 <https://doi.org/10.3809/jvirtex.2010.00223>. Paper 12, electronic edition.
- Cosentino, D., Asti, R., Nocentini, M., Gliozzi, E., Kotsakis, T., Mattei, M., Esu, D., Spadi, M., Tallini, M., Cifelli, F., Pennacchioni, M., Cavuoto, G., Di Fiore, V., 2017. New insights into the onset and evolution of the central Apennine extensional intermontane basins based on the tectonically active L'Aquila Basin (central Italy). *Geol. Soc. Am. Bull.* 129 (9–10), 1314–1336. <https://doi.org/10.1130/B31679.1>.
- Stratigrafia del Mesozoico e Cenozoico nell'area umbro-marchigiana. Itinerari geologici sull'Appennino umbro-marchigiano (Italia). In: Cresta, S., Monechi, S., Parisi, G. (Eds.), *Mem. Descr. Ila Carta Geol. Italia* 39, 182.
- Crone, A.J., Haller, K.M., 1991. Segmentation and the coseismic behavior of Basin and Range normal faults: examples from east-central Idaho and southwestern Montana. *J. Struct. Geol.* 13 (2), 151–164.
- De Paola, N., Collettini, C., Trippetta, F., Barchi, M.R., Minelli, G., 2007. A mechanical model for complex fault patterns induced by evaporites dehydration and cyclic fluid pressure increase. *J. Struct. Geol.* 29, 1573–1584.
- Di Bucci, D., Mazzoli, S., 2002. Active tectonics of the Northern Apennines and Adria geodynamics: new data and a discussion. *J. Geodyn.* 34 (5), 687–707. [https://doi.org/10.1016/S0264-3707\(02\)00107-2](https://doi.org/10.1016/S0264-3707(02)00107-2).
- Di Domenica, A., Turtù, A., Satolli, S., Calamita, F., 2012. Relationships between thrusts and normal faults in curved belts: new insight in the inversion tectonics of the Central-Northern Apennines (Italy). *J. Struct. Geol.* 42, 104–117. <https://doi.org/10.1016/j.jsg.2012.06.008>.
- Doglioni, C., Mongelli, F., Pieri, P., 1994. The Puglia uplift (SE Italy): an anomaly in the foreland of the Apenninic subduction due to buckling of a thick continental lithosphere. *Tectonics* 13 (5), 1309–1321. <https://doi.org/10.1029/94TC01501>.
- EMERGE Working Group, 2017. Photographic collection of the coseismic geological effects originated by the 24th August 2016, Amatrice (Central Italy) seismic sequence. *Miscellaneous INGV* 34, 1–114.
- Ercoli, M., Pauselli, C., Frigeri, A., Forte, E., Federico, C., 2014. 3-D GPR data analysis for high-resolution imaging of shallow subsurface faults: the Mt Vettore case study (Central Apennines, Italy). *Geophys. J. Int.* 198 (1), 609–621.
- Ferrarini, F., Lavecchia, G., de Nardis, R., Brozzetti, F., 2015. Fault geometry and active stress from earthquakes and field geology data analysis: the Colfiorito 1997 and L'Aquila 2009 Cases (Central Italy). *Pure Appl. Geophys.* 172 (5), 1079–1103.
- Ferrario, M.F., Livio, F., 2018. Characterizing the distributed faulting during the 30 October 2016, Central Italy earthquake: a reference for fault displacement hazard assessment. *Tectonics* 37, 1256–1273. <https://doi.org/10.1029/2017TC004935>.
- Finetti, J.R., Boccaletti, M., Bonini, M., Del Ben, A., Pipan, M., Prizzon, A., Sani, F., 2005. Lithospheric tectono-stratigraphic setting of the ligurian sea–northern apennines–adriatic foreland from integrated CROP seismic data. In: CROP PROJECT: Deep Seismic Exploration of the Central Mediterranean and Italy. Elsevier, pp. 119–158. Chapter: 8.
- Galadini, F., Galli, P., 2000. Active tectonics in the central apennines (Italy) – input data for seismic hazard assessment. *Nat. Hazards* 22 (3), 225–268. <https://doi.org/10.1023/A:1008149531980>.
- Galadini, F., Galli, P., 2003. Paleoseismology of silent faults in the central apennines (Italy): the Mt. Vettore and Laga mts. faults. *Ann. Geophys.* 46 (5).
- Galli, P., Galderisi, A., Peronace, E., Giaccio, B., Hajdas, I., Messina, P., Pileggi, D., Polpetta, F., 2019. The awakening of the dormant mount Vettore fault (2016 Central Italy earthquake, Mw 6.6): paleoseismic clues on its millennial silences. *Tectonics* 38 (2), 687–705.
- Giorgetti, C., Collettini, C., Scuderi, M., Barchi, M.R., Tesi, T., 2016. Fault geometry and mechanics of marly carbonate multilayers: an integrated field and laboratory study from the Northern Apennines, Italy. *J. Struct. Geol.* 93, 1–16. <https://doi.org/10.1016/j.jsg.2016.10.001>.
- Hampel, A., Li, T., Maniatis, G., 2013. Contrasting strike-slip motions on thrust and normal faults: implications for space-geodetic monitoring of surface deformation. *Geology* 41 (3), 299–302. <https://doi.org/10.1130/G33927.1>.
- Iezzi, F., Mildon, Z., Walker, J.F., Roberts, G.P., Goodall, H., Wilkinson, M., Robertson, J., 2018. Coseismic throw variation across along-strike bends on active normal faults: implications for displacement versus length scaling of earthquake ruptures. *J. Geophys. Res.: Solid Earth* 123, 9817–9841. <https://doi.org/10.1029/2018JB016732>.
- Improta, L., Latorre, D., Margheriti, L., Nardi, A., Marchetti, A., Lombardi, A.M., Castello, B., Villani, F., Ciaccio, M.G., Mele, F.M., Moretti, M., The Bollettino Sismico Italiano Working Group, 2019. Multi-segment rupture of the 2016 Amatrice-Visso-Norcia seismic sequence (central Italy) constrained by the first high-quality catalog of Early Aftershocks. *Sci. Rep.* 9 (1), 6921.
- Koopman, A., 1983. Detachment tectonics in the central Apennines, Italy. *Geol. Ultraiectina* 30, 1–55.
- Latorre, D., Mirabella, F., Chiaraluce, L., Trippetta, F., Lomax, A., 2016. Assessment of earthquake locations in 3-D deterministic velocity models: a case study from the Alotiberina Near Fault Observatory (Italy). *J. Geophys. Res.: Solid Earth* 121, 8113–8135. <https://doi.org/10.1002/2016JB013170>.
- Lavecchia, G., 1985. Il sovraccorrimiento dei Monti Sibillini: analisi cinematica e strutturale. *Boll. Soc. Geol. Ital.* 104, 161–194.
- Lavecchia, G., Brozzetti, F., Barchi, M.R., Menichetti, M., Keller, J.V.A., 1994. Seismotectonic zoning in east-central Italy deduced from an analysis of the Neogene to present deformations and related stress fields. *GSA Bulletin* 106 (9), 1107–1120. [https://doi.org/10.1130/0016-7606\(1994\)106<1107:SZIECI>2.3.CO;2](https://doi.org/10.1130/0016-7606(1994)106<1107:SZIECI>2.3.CO;2).
- Lavecchia, G., Castaldo, R., de Nardis, R., De Novellis, V., Ferrarini, F., Pepe, S., Brozzetti, F., Solaro, G., Cirillo, D., Bonano, M., Boncio, P., Casu, F., De Luca, C., Lanari, R., Manunta, M., Manzo, M., Pepe, A., Zinno, I., Tizzani, P., 2016. Ground deformation and source geometry of the 24 August 2016 Amatrice earthquake (Central Italy) investigated through analytical and numerical modeling of DInSAR measurements and structural-geological data. *Geophys. Res. Lett.* 43, 12,389–12,398. <https://doi.org/10.1002/2016GL071723>.
- Leonard, M., 2010. Earthquake fault scaling: self-consistent relating of rupture length, width, average displacement, and moment release. *Bull. Seismol. Soc. Am.* 100 (5A), 1971–1988. <https://doi.org/10.1785/0120090189>.
- Livio, F.A., Michetti, A.M., Vittori, E., Gregory, L., Wedmore, L., Piccardi, L., Tondi, E., Roberts, G., CENTRAL ITALY EARTHQUAKE, W.G., Blumetti, A.M., Bonadeo, L., Brunamonte, F., Comerci, V., Dimanna, P., Ferrario, M.F., Walker, J.F., Frigerio, C., Fumanti, G., Guerrieri, L., Iezzi, F., Leoni, G., McCaffrey, K., Mildon, Z., Phillips, R., Rhodes, E., Walters, R.J., Wilkinson, M., 2016. Surface faulting during the August 24, 2016, central Italy earthquake (Mw 6.0): preliminary results. *Ann. Geophys.* 59 (5) <https://doi.org/10.4401/ag-7197>.
- Ma, X.Q., Kusznir, N.J., 1995. Coseismic and postseismic subsurface displacements and strains for a dip-slip normal fault in a three-layer elastic gravitational medium. *J. Geophys. Res.* 100 (B7), 12,813–12,828.
- Mancinelli, P., Porreca, M., Pauselli, C., Minelli, G., Barchi, M.R., Speranza, F., 2019. Gravity and magnetic modeling of Central Italy: insights into the depth extent of the seismogenic layer. *Geochem. Geophys. Geosyst.* 20 (4), 2157–2172.
- Malinverno, A., Ryan, W.B.F., 1986. Extension in the Tyrrhenian Sea and shortening in the Apennines as result of arc migration driven by sinking of the lithosphere. *Tectonics* 5 (2), 227–245. <https://doi.org/10.1029/TC005i002p00227>.
- Mazzoli, S., Pierantoni, P.P., Borraccini, F., Paltrinieri, W., Deiana, G., 2005. Geometry, segmentation pattern and displacement variations along a major Apennine thrust zone, central Italy. *J. Struct. Geol.* 27 (11), 1940–1953. <https://doi.org/10.1016/j.jsg.2005.06.002>.
- Michetti, A.M., Ferrelli, L., Porfido, S., Blumetti, A.M., Vittori, E., Serva, L., Roberts, G.P., 2000. Ground effects during the 9 September 1998, Mw= 5.6 Lauria earthquake and the seismic potential of the “aseismic” Pollino region in southern Italy. *Seismol. Res. Lett.* 71 (1), 31–46. <https://doi.org/10.1785/gssrl.71.1.31>.
- Milli, S., Moscatelli, M., Stanzione, O., Falcini, F., 2007. Sedimentology and physical stratigraphy of the Messinian turbidite deposits of the Laga basin (central Apennines, Italy). *Boll. Soc. Geol. Ital.* 126 (2), 255.
- Milliner, C.W.D., Dolan, J.F., Hollingsworth, J., Leprince, S., Ayoub, F., Samsis, C.G., 2015. Quantifying near-field and off-fault deformation patterns of the 1992 Mw 7.3 Landers earthquake. *Geochem. Geophys. Geosyst.* 16, 1577–1598. <https://doi.org/10.1002/2014GC005693>.
- Mirabella, F., Ciaccio, M.G., Barchi, M.R., Merlini, S., 2004. The Gubbio normal fault (Central Italy): geometry, displacement distribution and tectonic evolution. *J. Struct. Geol.* 26 (12), 2233–2249. <https://doi.org/10.1016/j.jsg.2004.06.009>.
- Molli, G., 2008. Northern Apennine-Corsica orogenic system: an updated over-view. In: Siegesmund, B. Fugenschuh, Frotzheim, N. (Eds.), *Tectonic Aspects of the Alpine-Dinaride-Carpathian System*. Geological Society of London, pp. 413–442. Special Publication no. 298.

- Pantosti, D., Valensise, G., 1990. Faulting mechanism and complexity of the November 23, 1980, Campania-Lucania Earthquake, inferred from surface observations. *J. Geophys. Res.: Solid Earth* 95 (B10), 15319–15341. <https://doi.org/10.1029/JB095iB10p15319>.
- Patacca, E., Sartori, R., Scandone, P., 1990. Tyrrhenian basin and Apenninic arcs: kinematic relations since Late Tortonian times. *Mem. Soc. Geol. Ital.* 45, 425–451.
- Pauselli, C., Barchi, M.R., Federico, C., Magnani, M.B., Minelli, G., 2006. The crustal structure of the Northern Apennines (Central Italy): an insight by the CROP03 seismic line. *Am. J. Sci.* 306 (6), 428–450. <https://doi.org/10.2475/06.2006.02>.
- Peacock, D.C.P., Sanderson, D.J., 1991. Displacements, segment linkage and relay ramps in normal fault zones. *J. Struct. Geol.* 13 (6), 721–733.
- Peacock, D.C.P., Sanderson, D.J., 1992. Effects of layering and anisotropy on fault geometry. *J. Geol. Soc.* 149 (5), 793–802. <https://doi.org/10.1144/gsjgs.149.5.0793>.
- Perouse, E., Benedetti, L., Fleury, J., Rizza, M., Puliti, I., Billant, J., Pace, B., 2018. Coseismic slip vectors of 24 August and 30 October 2016 earthquakes in Central Italy: oblique slip and regional kinematic implications. *Tectonics* 37 (10), 3760–3781.
- Pierantoni, P.P., Deiana, G., Romano, A., Paltrinieri, W., Borraccini, F., Mazzoli, S., 2005. Geometrie strutturali lungo la thrust zone del fronte montuoso umbro-marchigiano-sabino. *Boll. Soc. Geol. Ital.* 124 (2), 395–411.
- Pierantoni, P.P., Deiana, G., Galdenzi, S., 2013. Stratigraphic and structural features of the sibillini mountains (Umbria–Marche apennines, Italy). *Italian Journal of Geosciences* 132, 497–520. <https://doi.org/10.3301/IJG.2013.08>.
- Pizzi, A., Scisciani, V., 2000. Methods for determining the Pleistocene–Holocene component of displacement on active faults reactivating pre-Quaternary structures: examples from the Central Apennines (Italy). *J. Geodyn.* 29 (3–5), 445–457. [https://doi.org/10.1016/S0264-3707\(99\)00053-8](https://doi.org/10.1016/S0264-3707(99)00053-8).
- Pizzi, A., Calamita, F., Coltorti, M., Pieruccini, P., 2002. Quaternary normal faults, intramontane basins and seismicity in the Umbria–Marche–Abruzzi Apennine Ridge (Italy): contribution of neotectonic analysis to seismic hazard assessment. *Bollettino della Società Geologica Italiana, Volume speciale n 11*, 923–929.
- Pizzi, A., Galadini, F., 2009. Pre-existing cross-structures and active fault segmentation in the northern-central Apennines (Italy). *Tectonophysics* 476 (1–2), 304–319. <https://doi.org/10.1016/j.tecto.2009.03.018>.
- Pizzi, A., Di Domenica, A., Gallovič, F., Luzi, L., Puglia, R., 2017. Fault segmentation as constraint to the occurrence of the main shocks of the 2016 Central Italy seismic sequence. *Tectonics* 36, 2370–2387. <https://doi.org/10.1002/2017TC004652>.
- Porreca, M., Minelli, G., Ercoli, M., Brobia, A., Mancinelli, P., Cruciani, F., Giorgetti, C., Carbone, F., Mirabella, F., Cavinato, G., Cannata, A., Pauselli, C., Barchi, M.R., 2018. Seismic reflection profiles and subsurface geology of the area interested by the 2016–2017 earthquake sequence (Central Italy). *Tectonics* 37, 1116–1137. <https://doi.org/10.1002/2017TC004915>.
- Pucci, S., De Martini, P.M., Pantosti, D., Valensise, G., 2003. Geomorphology of the Gubbio Basin (Central Italy): understanding the active tectonics and earthquake potential. *Ann. Geophys.* 46 (5).
- Pucci, S., De Martini, P.M., Civico, R., Villani, F., Nappi, R., Ricci, T., Azzaro, R., Brunori, C.A., Caciagli, M., Cinti, F.R., Sapia, V., De Ritis, R., Mazzarini, F., Tarquini, S., Gaudiosi, G., Nave, R., Alessio, G., Smedile, A., Alfonsi, L., Cucci, L., Pantosti, D., 2017. Coseismic ruptures of the 24 August 2016, Mw 6.0 Amatrice earthquake (Central Italy). *Geophys. Res. Lett.* 44 (5), 2138–2147. <https://doi.org/10.1002/2016GL071859>.
- Roberts, G.P., 1996. Variation in fault-slip directions along active and segmented normal fault systems. *J. Struct. Geol.* 18 (6), 835–845. [https://doi.org/10.1016/S0191-8141\(96\)80016-2](https://doi.org/10.1016/S0191-8141(96)80016-2).
- Roberts, G.P., Ganas, A., 2000. Fault-slip directions in central and southern Greece measured from striated and corrugated fault planes: comparison with focal mechanism and geodetic data. *J. Geophys. Res.* 105 (B10), 23443–23462. <https://doi.org/10.1029/1999jb900440>.
- Roberts, G.P., Michetti, A.M., 2004. Spatial and temporal variations in growth rates along active normal fault systems: an example from the Lazio–Abruzzo Apennines, central Italy. *J. Struct. Geol.* 26 (2), 339–376. [https://doi.org/10.1016/S0191-8141\(03\)00103-2](https://doi.org/10.1016/S0191-8141(03)00103-2).
- Royden, L., Patacca, E., Scandone, P., 1987. Segmentation and configuration of subducted lithosphere in Italy: an important control on thrust-belt and foredeep-basin evolution. *Geology* 15 (8), 714–717. [https://doi.org/10.1130/0091-7613\(1987\)15<714:SACOSL>2.0.CO;2](https://doi.org/10.1130/0091-7613(1987)15<714:SACOSL>2.0.CO;2).
- Sage, L., Mosconi, A., Moretti, I., Riva, E., Roure, F., 1991. Cross section balancing in the central apennines: an application of locace (1). *AAPG (Am. Assoc. Pet. Geol.) Bull.* 75 (4), 832–844.
- Santantonio, M., 1994. Pelagic carbonate platforms in the geologic record: their classification, and sedimentary and paleotectonic evolution. *AAPG (Am. Assoc. Pet. Geol.) Bull.* 78 (1), 122–141. <https://doi.org/10.1306/BDF9032-1718-11D7-8645000102C1865D>.
- Scarsella, F., 1941. Carta geologica d'Italia, in scala 1:100.000. Foglio 132 (Norcia). Fault segmentation and controls of rupture initiation and termination. In: Schwartz, D.P., Sibson, R.H. (Eds.), *United States Geological Survey-Open-File Report* 89–315, 1–447.
- Scisciani, V., Agostini, S., Calamita, F., Pace, P., Cilli, A., Giori, I., Paltrinieri, W., 2014. Positive inversion tectonics in foreland fold-and-thrust belts: a reappraisal of the Umbria–Marche Northern Apennines (Central Italy) by integrating geological and geophysical data. *Tectonophysics* 637, 218–237.
- Scognamiglio, L., Tinti, E., Casarotti, E., Pucci, S., Villani, F., Cocco, M., Magnoni, F., Michelini, A., Dreger, D., 2018. Complex fault geometry and rupture dynamics of the Mw 6.5, 2016, October 30th central Italy earthquake. *J. Geophys. Res.: Solid Earth* 123, 2943–2964. <https://doi.org/10.1002/2018jb015603>.
- Stirling, M., Goded, T., Berryman, K., Litchfield, N., 2013. Selection of earthquake scaling relationships for seismic-hazard analysis. *Bull. Seismol. Soc. Am.* 103 (6), 2993–3011. <https://doi.org/10.1785/0120130052>.
- Tavani, S., Storti, F., Salvini, F., Toscano, C., 2008. Stratigraphic versus structural control on the deformation pattern associated with the evolution of the Mt. Catria anticline, Italy. *J. Struct. Geol.* 30 (5), 664–681.
- Teran, O.J., Fletcher, J.M., Oskin, M.E., Rockwell, T.K., Hudnut, K.W., Spelz, R.M., Akciz, S.O., Hernandez-Flores, A.P., Morelan, A.E., 2015. Geologic and structural controls on rupture zone fabric: a field-based study of the 2010 Mw 7.2 El Mayor–Cucapah earthquake surface rupture. *Geosphere* 11 (3), 899–920. <https://doi.org/10.1130/GES01078.1>.
- Tinti, E., Scognamiglio, L., Michelini, A., Cocco, M., 2016. Slip heterogeneity and directivity of the ML 6.0, 2016, Amatrice earthquake estimated with rapid finite-fault inversion. *Geophys. Res. Lett.* 43 (20), 10,745–10,752. <https://doi.org/10.1002/2016GL071263>.
- Tung, S., Masterlark, T., 2018. Resolving source geometry of the 24 August 2016 Amatrice, Central Italy, earthquake from InSAR data and 3D finite-element modeling. *Bull. Seismol. Soc. Am.* 108 (2), 553–572. <https://doi.org/10.1785/0120170139>.
- Villani, F., Pucci, S., Civico, R., De Martini, P.M., Cinti, F.R., Pantosti, D., 2018a. Surface faulting of the 30 October 2016 Mw 6.5 central Italy earthquake: detailed analysis of a complex coseismic rupture. *Tectonics* 37, 3378–3410. <https://doi.org/10.1029/2018TC005175>.
- Villani, F., Sapia, V., Baccheschi, P., Civico, R., Di Giulio, G., Vassallo, M., Marchetti, M., Pantosti, D., 2018b. Geometry and structure of a fault-bounded extensional basin by integrating geophysical surveys and seismic anisotropy across the 30 October 2016 Mw 6.5 earthquake fault (central Italy): the Pian Grande di Castelluccio basin. *Tectonics* 38, 26–48. <https://doi.org/10.1029/2018TC005205>.
- Walters, R.J., Gregory, L.C., Wedmore, L.N.J., Craig, T.J., McCaffrey, K., Wilkinson, M., Chen, J., Li, Z., Elliott, J.R., Goodall, H., Iezzi, F., Livio, F., Michetti, A.M., Roberts, G.P., Vittori, E., 2018. Dual control of fault intersections on stop-start rupture in the 2016 Central Italy seismic sequence. *Earth Planet. Sci. Lett.* 500, 1–14. <https://doi.org/10.1016/j.epsl.2018.07.043>.
- Wells, D.L., Coppersmith, K.J., 1994. New empirical relationships among magnitude, rupture length, rupture width, rupture area, and surface displacement. *Bull. Seismol. Soc. Am.* 84 (4), 974–1002.
- Wilkinson, M.W., McCaffrey, K.J.W., Jones, R.R., Roberts, G.P., Holdsworth, R.E., Gregory, L.C., Walters, R.J., Wedmore, L., Goodall, H., Iezzi, F., 2017. Near-field fault slip of the 2016 Vettore Mw6.6 earthquake (Central Italy) measured using low-cost GNSS. *Sci. Rep.* 7, 4612. <https://doi.org/10.1038/s41598-017-04917-w>.
- Xu, G., Xu, C., Wen, Y., Jiang, G., 2017. Source parameters of the 2016–2017 Central Italy earthquake sequence from the Sentinel-1, ALOS-2 and GPS data. *Remote Sens.* 9 (11), 1182. <https://doi.org/10.3390/rs9111182>.
- Zinke, R., Hollingsworth, J., Dolan, J.F., 2014. Surface slip and off-fault deformation patterns in the 2013 MW 7.7 Balochistan, Pakistan earthquake: implications for controls on the distribution of near-surface coseismic slip. *Geochem. Geophys. Geosyst.* 15, 5034–5050. <https://doi.org/10.1002/2014GC005538>.